Warm Cumulus Cloud Seeding Potential

By

Richard Durham

Department of Atmospheric Science
Colorado State University
Fort Collins, Colorado

Colorado State University

Department of Atmospheric Science

Paper No. 202

WARM CUMULUS CLOUD SEEDING POTENTIAL

by

Richard Durham

This report was prepared with support provided by
National Science Foundation Grant
No. GI-31460

Department of Atmospheric Science
Colorado State University
Fort Collins, Colorado

July, 1973

Atmospheric Science Paper No.

WARM CUMULUS CLOUD SEEDING POTENTIAL

A one-dimensional steady-state cumulus model is described. The model considers the processes of lateral entrainment, droplet growth by condensation and coalescence, droplet freezing and the development and fallout of precipitation, as well as the standard thermodynamic and dynamic processes in isolated cumuli. The numerical model is reviewed and comparisons are made between model predicted cloud characteristics and observations made during a cumulus modification program conducted near Rapid City, South Dakota in the summer months of 1969-1971. The model is used to evaluate the importance of the warm coalescence process and the climatological potential for rainfall augmentation through sodium chloride seeding of isolated cumulus clouds on the Great Plains. The model shows that coalescence plays an important role in the natural formation of rain in the south-eastern portions of the Great Plains, but is of minor importance in the more continental areas. Rainfall could be initiated by sodium chloride seeding in all areas of the Great Plains. In the southern portions of the Great Plains significant amounts of rain could be produced in clouds that are unsuitable for other forms of seeding.

ACKNOWLEDGEMENTS

The author expresses his sincere appreciation to Professor Lewis O. Grant for his valuable suggestions and encouragement throughout the various aspects of this work. The author is also indebted to Professor Michael Corrin for his many helpful discussions and to Dr. James Dye for his critical reviews of the manuscript.

Special thanks go to Dave Blanchar and Dean Purdy who worked many hours on the data reduction and programming. Special thanks are also given to Beryl Younkin who typed the many revisions of the manuscript.

This research was sponsored in part by the National Science Foundation, Grant No. GI-31460.

TABLE OF CONTENTS

LIST OF TABLES

LIST OF FIGURES

INTRODUCTION

Since the first dramatic results of cloud modification by dry ice seeding in 1947, the possibility of economically increasing precipitation in cold clouds has been viewed with optimism. The discovery that silver iodide could be used as a simple and economic cloud-seeding agent hastened the progress in this area. Now that the seeding of some cold orographic clouds is considered to be in an operational stage, greater research emphasis is now being placed on the potential benefits of warm cloud modification.

The seeding techniques applied to warm clouds are less developed than those applied to cold clouds. Numerical modeling of the warm precipitation mechanism can lead to an increased understanding of the interrelationship between cloud physics processes and the precipitation mechanism. A numerical model can predict the effect of the modification upon more than one measurable quantity, thus increasing our power to test the validity of the modification hypothesis.

The purpose of this paper is to describe a numerical model for droplet growth in a cumulus cloud and utilize this model to study the warm rain process and the potential for precipitation augmentation by hygroscopic seeding in various areas of the Great Plains. Cloud physics processes are realistically simulated by simple mathematics. Input data required for the model includes a vertical profile of pressure, temperature, relative humidity, and horizontal wind speed. Initial conditions at cloud base of updraft velocity, updraft radius, cloud radius, and droplet spectrum are also required. During a field research program, the initial conditions at cloud base can be determined by aircraft observation.

The numerical model presented here utilizes the laws of thermodynamics, the third equation of motion and several qualitative and empirical expressions that describe the warm precipitation process. The result is a numerical model that requires little computer storage space and permits rapid, economical calculations.

The model simulates the growth of raindrops in the updraft region of a cumulus. The raindrop embryos* grow by condensation and by coalescence with a dense population of uniform cloud droplets. The initial droplet spectrum approximates actual observations found in cumulus clouds in the general area of the radiosonde stations used. Updraft radius, velocity and temperatures are calculated at each time step as well as droplet concentration, liquid water content, supersaturation and drop growth.

The raindrop is initially carried up by the updraft, but then begins to fall relative to the air. Water loading decreases buoyancy and eventually downdrafts form. Once the air begins to move downward there is an additional decrease in buoyancy due to the air cooling at near the moist adiabatic rate and consequent development of a temperature deficit with respect to the environment.

The model will predict if rainfall can occur by natural warm processes and if it can be produced through hygroscopic seeding. It also predicts rainfall amounts and estimates the efficiency of the warm precipitation mechanism.

---

*The term raindrop embryos is used here to designate those drops that grow much more rapidly than the average drop, and have the best chance to develop into precipitation before being ejected from cloud top.

THE MODEL

The model treated here and in the succeeding section can be thought of as two different physical models in one. The first model is the steady-state jet model that can be traced to the work of Weinstein and Davis (1968) Squires and Turner (1962), and originating with the work of Stommel (1947). The second model simulates the growth of raindrops within the cloud. The basis for this portion of the model was established by Bowen (1950).

1. Entrainment

Namias (1939) attributed the dissipation of tall cumulus clouds to the mixing of dry environmental air into the cloud. This mixing, or entrainment as it is usually referred to, is now recognized as the single most destructive process for isolated cumulus clouds.

The entrainment rate has been shown to be inversely related to the updraft radius (Squires and Turner, 1962),

$$\mu = \frac{1}{M}\frac{dM}{dz} = \frac{2\alpha}{A} \qquad (1)^*$$

where α is the proportionality constant relating the inflow velocity at the edge of the plume to the vertical velocity within it. The difference in density between the environment and the cloud is neglected.

The entrainment rate for momentum and temperature is determined by the updraft radius since the greatest gradients for these parameters occur at the edge of the updraft core (Fig. 1). By similar reasoning the entrainment rate for moisture is determined by the physical cloud radius.

---

*Symbols for this and all following equations can be found in Appendix A.

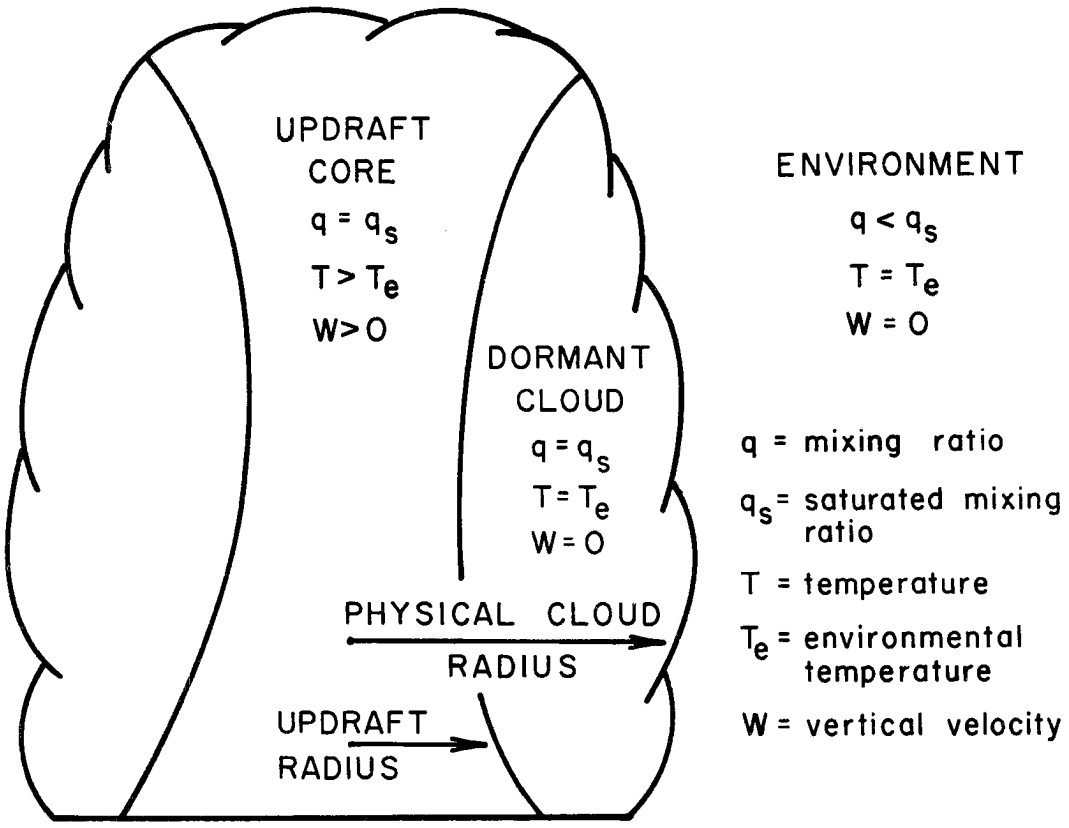

Fig. 1 Schematic diagram of an isolated cumulus cloud (after Weinstein 1968).

2. Updraft Radius

Mass continuity within the updraft requires that the updraft radius vary with height.

The mass flux through the core is,

$$M = \pi A^2 \rho W \tag{2}$$

and the change with height is

$$\frac{dM}{dz} = 2\pi A \alpha W \rho_e \tag{3}$$

where ρ_e is the density of the environment.

By taking the total derivative of z as a function of A, W and ρ,

$$dz = (\partial z/\partial A)dA + (\partial z/\partial W)dW + (\partial z/\partial \rho)d\rho \tag{4}$$

and then dividing through by dz and solving for the change in updraft radius with height it is found that,

$$dA/dz = (\rho_e/\rho)\alpha - \frac{A}{2}\left[\frac{1}{W}\frac{dW}{dz} + \frac{1}{\rho}\frac{d\rho}{dz}\right] \tag{5}$$

or

$$\frac{dA}{dz} \approx \alpha - \frac{A}{2}\left[\frac{1}{W}\frac{dW}{dz} + \frac{1}{\rho}\frac{d\rho}{dz}\right] . \tag{6}$$

Since

$$\rho_e/\rho \approx 1$$

it is apparent from (6) that if the updraft velocity increases with height faster than the density decreases, and if entrainment does not provide sufficient mass to make up the difference, then the updraft radius must decrease. When the updraft velocity decreases the updraft radius must increase. This results in the typical updraft profile depicted in Fig. 1.

3. Thermodynamics

The first law of thermodynamics is used to calculate the change in temperature with height.

$$-\frac{dT}{dz} = \frac{g/C_p\left[1 + \frac{q_s L}{R_d T}\right] + \mu[T-T_e] + \frac{\mu L}{C_p}(q_s - q_e) + \frac{Lf}{C_p}\frac{(q_f)}{dz}}{1 + \frac{\varepsilon L^2 q_s}{C_p R_d T^2}} \tag{7}$$

The terms on the right side of (7) represent (from left to right) the moist adiabatic temperature decrease, the temperature change caused by the heat lost to warm the entrained air and the heat gained from the latent heat of fusion.

In cloud measurements of solid and liquid-water content are rare in cumulus clouds above the -10C level. The scanty information that is

available indicates that in the updraft region ice constitutes a very small amount of the total water mass at temperatures warmer than -20C. Foreign ice nuclei are required to freeze the cloud droplets at temperatures warmer than -40C. At -20C these nuclei are available in concentrations of about one per liter. The concentration of ice nuclei increases by a factor of ten for approximately every 4C decrease in temperature. This would indicate an exponential relationship between temperature and percent of cloud water frozen. The cloud water would be completely frozen through homogeneous nucleation at -40C. The relationship of percent of water in the solid state to temperature used by the numerical model is illustrated by Fig. 2.

4. Moisture Balance

The saturation vapor pressure was calculated from the empirical equation (Betts and Dugan, 1973),

$$E_W = 6.11 \times 10^{\left(\frac{7.5T}{T+237.3}\right)} \quad T(^{o}C) \tag{8}$$

This equation is accurate within 1% over the range from +20C to -25C.

The mixing ratio was calculated from

$$q = (0.622E_W) \; / \; (P-E_W) \; . \tag{9}$$

No correction is made for the departure of the mixture of air and water vapor from the ideal gas laws.

The liquid water content of the cloud is comprised of cloud droplets and hydrometeor sized drops.

$$\omega = \omega_c + \omega_H \tag{10}$$

The contribution of the cloud droplets is calculated from the equation

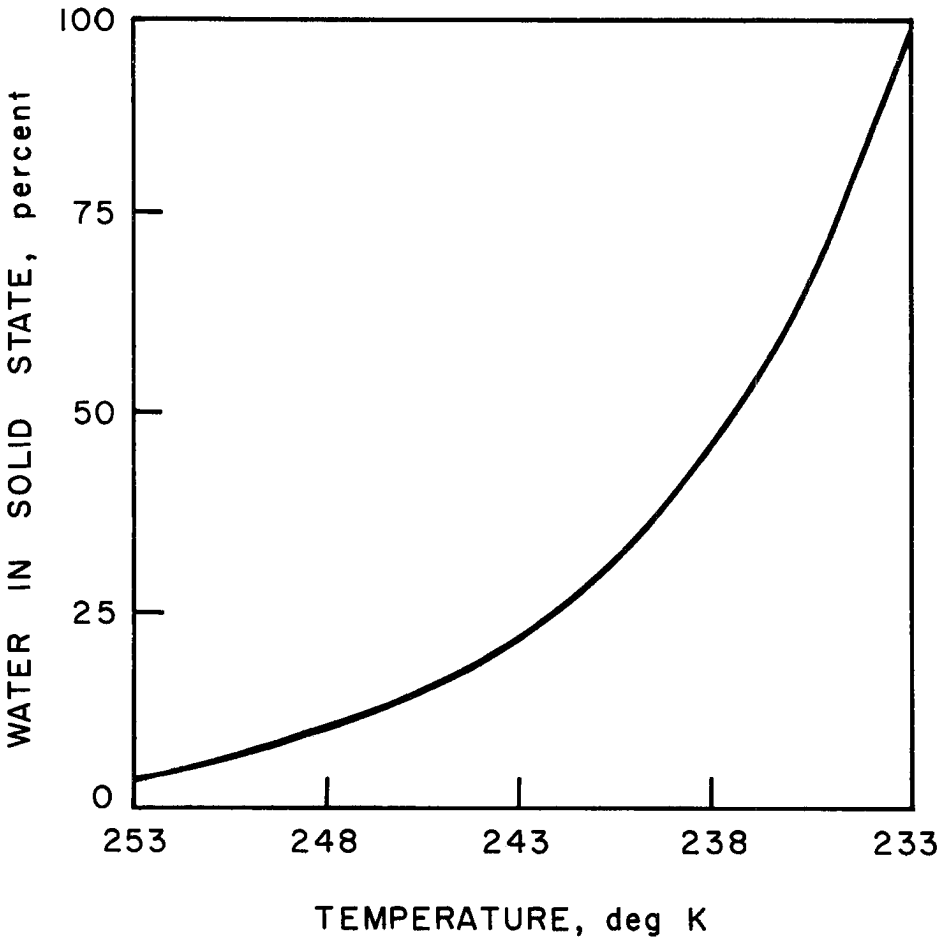

Fig. 2 The percent of water in the solid state in relation to temperature in the updraft portion of an isolated cumulus cloud.

$$\omega_c = [\omega_c' + (q_s' - q_s)][1/(1+\mu dz)] - \mu dz\ (q_s - q_e) \qquad (11)$$

where ω_c' and q' are the liquid water content and mixing ratio calculated by the model during the previous time step.

The first term on the right side of (11) represents the addition of liquid water due to condensation. This is multiplied by a factor to compensate for the increased volume in the updraft due to entrainment. The second term represents the amount of liquid water required to saturate the entrained environmental air.

The liquid-water content contributed by the large drops per gram of air was simply the volume of the drops times the number of drops per gram of air. The density of water was taken to be 1.

5. Dynamics

The third equation of motion can be written as,

$$\frac{dW}{dt} = -\frac{1}{\rho}\frac{dP}{dz} - g - \text{drag} \quad . \tag{12}$$

Assuming that the drag force is due to the weight of liquid water and the transfer to momentum from the updraft to entrainment air of the dormant cloud, (12) can be rewritten as

$$\frac{dW}{dt} = -\frac{1}{\rho} - g - \omega g - \mu W^2 \quad . \tag{13}$$

If it is assumed that there is no horizontal pressure gradient and the environment is in hydrostatic equilibrium then (13) becomes

$$\frac{dW}{dt} = \left(\frac{\rho_e - \rho}{\rho}\right) g - \omega g - W^2 \quad . \tag{14}$$

By substituting the ideal gas law into (14), using the virtual temperature, the final form of the vertical motion equation is arrived at,

$$\frac{dW}{dt} = \left[\frac{T_v - T_{vE}}{T_v}\right] g - \omega g - W^2 \quad . \tag{15}$$

The terms on the right of (15) represent buoyant acceleration, deceleration due to water loading and deceleration due to the entrainment of stationary cloud or environmental air.

A correction is made to the buoyancy equation based on laboratory results of Turner (1963). Turner describes a virtual mass effect in which the rising plume loses momentum to the environment as a result

of the "pushing" of the environmental air on the plume. For use in the numerical model the value of σ, the virtual mass coefficient, is taken to be 0.5, similar to Simpson and Wiggert (1969). Equation (15) is now

$$\frac{dW}{dt} = \left[\frac{T_v - T_{vE}}{T_v}\right] - \omega \frac{g}{1+\sigma} - \mu W^2 \quad . \tag{16}$$

The vertical velocity can then be calculated from

$$W_2 = W_1 + \frac{dW}{dt}\, dt \tag{17}$$

where W_1 is the vertical velocity calculated at the previous time step.

A second correction made to the updraft velocity due to horizontal wind shear, is based on the relationship given by Malkus (1952). The adjusted vertical velocity is the vertical component of the updraft given by (17). The true vertical velocity can be calculated from

$$W = [W_2^2 - (U-U_o)^2]^{0.5} \quad . \tag{18}$$

U can be calculated by considering the horizontal momentum in the updraft before and after entrainment of environmental air.

$$U = \frac{U_1 + \mu dz U_E}{1 + \mu dz} \quad . \tag{19}$$

Substituting the above into (18) yields

$$W = [W_1^2 = (\frac{U_1 + \mu dz U_E}{1 + \mu dz} - U_o)^2]^{0.5} \quad .$$

6. Precipitation

The most difficult part of simulating raindrop growth is that of precipitation fallout. Simpson and Wiggert (1969) proposed a simple

method for determining that portion of water that is to fall out as rain. Simpson and Wiggert took the fractional fallout of precipitation in each vertical integration as the ratio of the time for the tower to rise through a vertical depth, Δz, to the time for the median-volume diameter drop to fall the distance of one radius of the rising spherical cloud bubble. This fallout scheme is conceptually inconsistent with the steady state jet model presented here.

Weinstein and Davis (1968) proposed that all precipitation should be released from a steady-state jet when the terminal velocity of the median-volume diameter drop exceeded the updraft velocity. This caused the precipitation to be carried upward until the updraft was nearly destroyed. This resulted in liquid-water contents that were too high in the upper portions of the cloud. In the PSU (Pennsylvania State University) model precipitation released at any level has no effect on the cloud below. One consequence of this is that the PSU model describes only upward-directed vertical motions with no consideration given to downdrafts. In the model presented here the major drawback is that the droplet spectrum is comprised of only two size drops; rain embryos that grow by both condensation and coalescence and a constant number of uniform cloud droplets. The advantage is that the growth of the raindrops can be followed throughout the cumulus and mature stage of the cloud.

The waterloading factor in (15) is due to the liquid water condensed in the parcel and to raindrops that have fallen into the parcel from above. Precipitation transfers water from the upper portions of the cloud downward. If the water loading factor exceeds the buoyancy, due to the temperature excess of the updraft, a downdraft is formed.

7. Cloud Base Determination

Cloud base height is calculated as the convective condensation level using the observed mixing ratio 200m above the surface.

The vapor pressure of water in the parcel is calculated from

$$E_W = (E'_W + E_{We} \cdot \mu \cdot dz) \; / \; (1.0 + \mu \cdot dz) \quad . \tag{20}$$

The temperature at which E_W is equal to the saturation vapor pressure can be found by solving the integrated form of the Clausius-Clapeyron equation for T.

$$T = (-R/m_W \cdot L) \quad \ln (E_W/6.11) + 1.0/273.0 \quad . \tag{21}$$

When the vapor pressure of water in the parcel exceeds the saturation vapor pressure of water in the environment condensation is assumed to occur and cloud base is determined.

DROPLET GROWTH

The approximate equation of growth by diffusion is:

$$R\frac{dR}{dt} = G(S - \frac{a}{R} + \frac{b}{R^3})f(R_e,P_r') \tag{22}$$

where S is the natural supersaturation and a and b are constants related to the effect of curvature and solution on the vapor pressure. The function $f(R_e,P_r')$ is due to the ventilation of the drops as they fall relative to their environment and G is a thermodynamic function of temperature and pressure (Fletcher, 1966).

$$G = \frac{D\rho_V}{\rho_L}\left[1 + \frac{DL^2P_Vm_Wf(R_e,P_r')}{RT^2\kappa f(R_e,P_r)}\right]^{-1} \tag{23}$$

Equation (22) can be rewritten as

$$R\frac{dR}{dt} = G(S+S'(R)) \ . \tag{24}$$

The increase in saturation over the drop due to the solution effect is now represented by S'. The ventilation factor, which tends to increase the rate of growth has been neglected. This has been shown to be a good approximation for droplets less than 30μ in radius (Squires, 1952). For larger droplets, growth is dominated by processes other than condensation. The effect of curvature is also considered negligible.

In a large population of droplets growing in an updraft by condensation, there is very little interaction among the individual droplets. Every growing droplet experiences essentially the same environment, and they influence each other only through their combined effect on their common environment.

The number and size of the droplets is determined at cloud base by the condensation nuclei available. The supersaturation increases rapidly and reaches a peak within a hundred meters of cloud base. This peak supersaturation is reduced by condensation on the rapidly growing liquid surfaces. After this phase of droplet growth the rate of condensation approaches the rate at which water vapor becomes available. It is at this point, when the droplets are well passed the activation stage, that the natural supersaturation can be calculated by the relation given by Squires (1952).

$$S \approx (0.0239W + 1.72 \times 10^{-6} n)/\Sigma r \qquad (25)$$

where:

S = Supersaturation expressed as an elevation of the dew point in ^{o}C

W = Updraft velocity in cms^{-1}

n = Number of droplets per gram of air

Σr = Sum of the radii of droplets per gram of air.

Raoult's law can be used to estimate the supersaturation due to the solution effect. The vapor pressure of water over a solution can be related to the concentration of solute through the equation

$$P' = PX \quad , \qquad (26)$$

where P' is the vapor pressure of water over the plane surface of a solution containing a mole fraction, X, of water. P is the vapor pressure over pure water. Raoult's law works well for sodium chloride solutions of mole fractions of water greater than .91, but at greater concentrations of salt the percentage decrease in vapor pressure predicted by Raoult's law is too small. For calculating supersaturations

to be used in computing droplet growth, a correction factor must be added at these higher concentrations (Fig. 3).

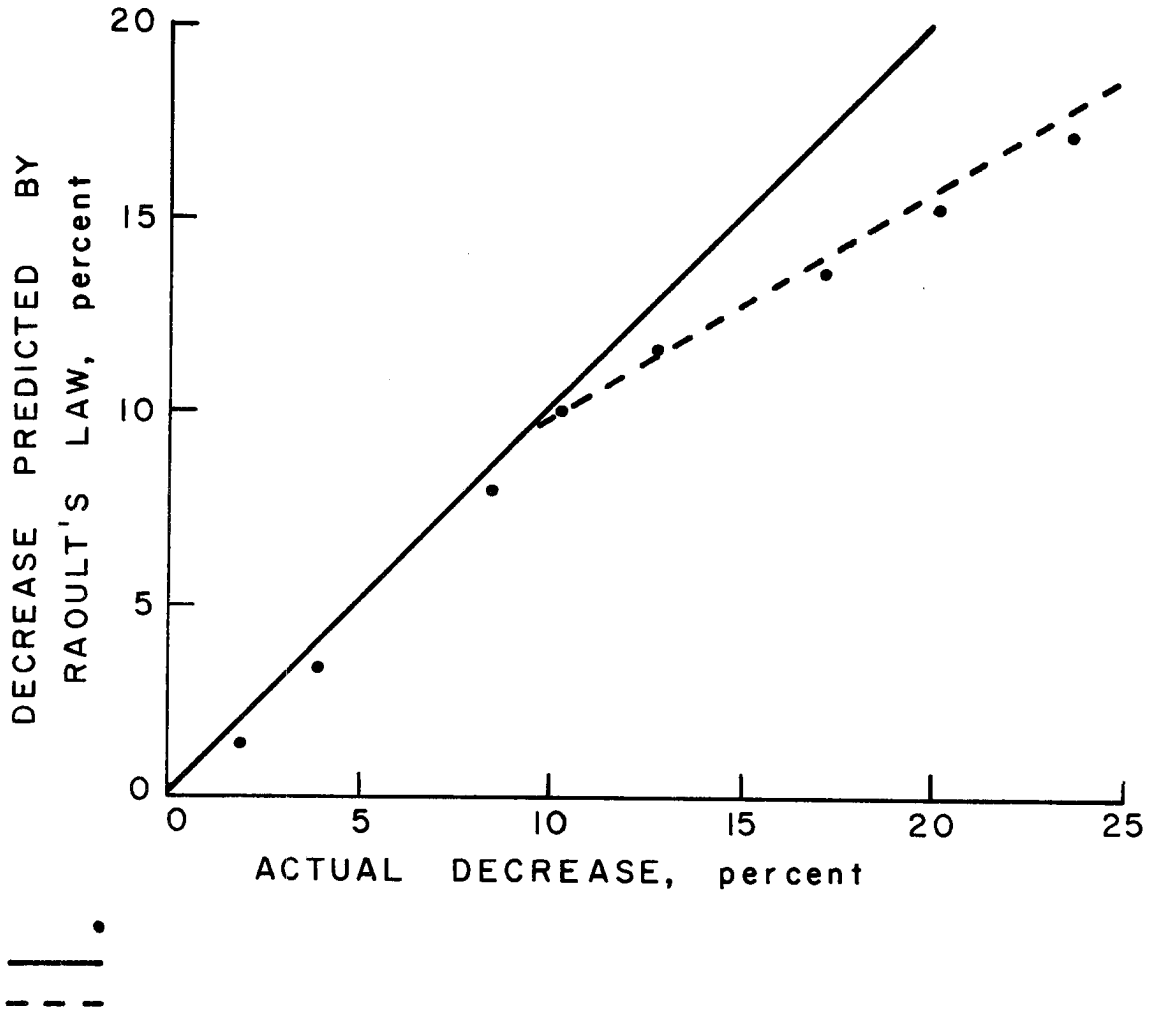

Fig. 3 Correction to Raoult's law used by the model.

After a droplet reaches a radius of 50μ it grows rapidly by colliding with and cohering to cloud droplets. The rate of growth is dependent upon the size and number of cloud droplets that are struck during a period of time and the efficiency with which they coalesce. In a cloud, the larger drops are falling relative to the smaller droplets. The number of droplets swept out per unit time is dependent upon

the difference in terminal velocities between the large and small drops and the radius of the large drop.

The terminal velocities of raindrops were determined by Gunn and Kinzer (1949). The computer model used a polynomial equation developed by Dingle and Lee (1972) to calculate terminal velocities. This numerical expression fits the velocities determined by Gunn and Kinzer within a maximum error of 0.7%. The terminal velocities of cloud droplets, radii less than 50μ, were calculated from Stokes law. A correction has been applied for the effect of air density on terminal fall speed.

For a water drop falling at its terminal velocity in air, the balance of forces can be represented by

$$mg = \frac{1}{2} V^2 C_D R^2 \tag{27}$$

where the left side of the equation represents the gravitational force on the drop and the right side is the upward directed aerodynamic drag.

For a drop of a given size a correction for air density is given by (28).

$$V = V_o [\frac{\rho_o}{\rho}]^{0.4} \tag{28}$$

where V_o is the terminal velocity at air density ρ_o and V is that at ρ. If a given drop had the same drag coefficient at different air densities, (27) indicates that the exponent in (28) should be 0.5. However, Foote and DuToit (1969) showed that the exponent of 0.4 is more accurate because of higher drag coefficients at lower air densities.

There are two coalescence growth models in use today. These models are distinguished from each other by the relative amount of

water gathered from the various sizes of smaller droplets by the larger drops. The continuous model calculates only the averaged and smoothed rate of growth of all drops of a given radius. The continuous model assumes that small droplets are swept out as if their mass were distributed uniformly in space. All large drops would grow at the same rate. In the stochastic model water is gathered from drops of all sizes. This is important because a chance capture of a large drop can increase mass greater than the capture of one hundred small droplets. The stochastic model allows the large drops to grow at different rates causing the drop size distribution to spread (Fig. 4).

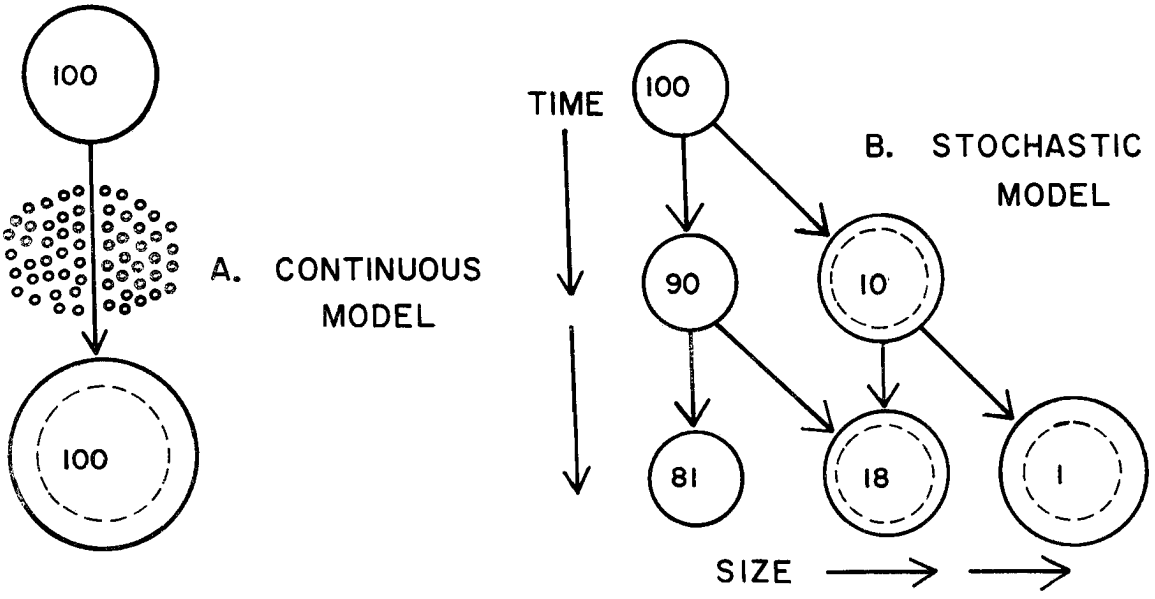

Fig. 4 A schematic diagram illustrating the differences between the continuous and stochastic growth concepts (adapted from Berry 1967).

In nature the precipitation mechanism is a discrete and stochastic process. Here, however, realism must yield to economics. The stochastic process requires too much computer time to be used in a model

that is to be run for numerous cases. Since the continuous model requires very little computer time and because it is well suited to simulate the behavior of a few relatively large drops growing within a dense population of smaller droplets, it was deemed appropriate for this model.

The growth of the droplets following the continuous model can be calculated from

$$\frac{dR}{dt} = \frac{\pi}{3} \int_0^R n(r) r^3 E'(R,r)[V(R) - V(r)]dr \qquad (29)$$

where $n(r)$ is the number of droplets per unit volume of air with radii between r and $r + dr$, $V(R)$ and $V(r)$ are the terminal velocities of the larger drops and small droplets of radii R and r respectively. The collection cross-section for the two different droplets is $E'(R,r)$. E' is related to the collection efficiency E, by the equation

$$E' = E(R+r)^2/R^2 \qquad (30)$$

The collection efficiency is the product of the collision efficiency and the coalescence efficiency. The coalescence efficiency is assumed to be unity. Collision efficiencies are taken from Davis and Klett (1973) for $R < 45\mu$, from Shafrir and Neiburger (1963) for $45\mu \leq R \leq 100\mu$ and from Fonda and Herne (1957) for $R > 100\mu$.

In the simple case where all of the small droplets are of uniform size and constitute a liquid water content of ω grams per cubic centimeter, then (29) reduces to,

$$\frac{dR}{dt} = \frac{E'(R,r)}{4\rho_L}\,\omega(V(R) - V(r)) \tag{31}$$

where ρ_L is the density of liquid water.

A correction has been added to the continuous growth equation for unseeded cases to simulate the faster growth of raindrops in the stochastic model. As indicated by the stochastic model, some drops grow at a rate much more rapid than average. It is these faster growing drops that eventually produce precipitation. Telford (1955) used a discrete size distribution to demonstrate mathematically that the stochastic model produced relatively large drops approximately six times as fast as the continuous equation.

Berry (1967) confirmed the calculations made by Telford. Berry considered only the larger drops that had a concentration of $10m^{-3}$ at $t = 0$. Berry's calculations showed that these drops doubled in mass every 100 seconds. That is

$$\frac{dm}{dt}\ (\text{stochastic}) = \frac{m}{50}\ . \tag{32}$$

Continuous growth takes place at the rate,

$$\frac{dm}{dt}\ (\text{continuous}) = mbw \approx \frac{m}{300} \tag{33}$$

where b, a constant in the collection kernel, has a value of $\approx 3 \times 10^{-3}\ (m^3 gm^{-1} sec^{-1})$. It follows that

$$\frac{dm}{dt}\ (\text{stochastic})/\frac{dm}{dt}\ (\text{continuous}) \approx 6 \tag{34}$$

demonstrating that Berry's calculations agree with Telford's for the few larger drops at the beginning of collection growth for $R < 45\mu$.

To simulate the faster growth of a few favored drops, the raindrop embryos were allowed to grow at six times the continuous rate until a radius of 45μ was reached.

1. Adjustment to Liquid Water Content

The first drop to fall through a layer of cloud will encounter a liquid water content equal to the amount of water vapor condensed in that layer since rising from cloud base. For all drops thereafter the liquid water content will be decreased by that amount which has coalesced with and has been transported out of the layer by previous raindrops.

A short numerical model (Appendix B) was developed to study the effect that this process had on the liquid water content encountered by the average drop. (The average drop is that drop increasing in mass at a rate that is the average for all drops.)

It was determined that the percent of liquid water made available to the average drop was mainly a function of drop radius and number. An expression was included in the numerical cloud model to account for this phenomenon.

2. Drop Breakup

Since drops of radius greater than 2.5mm are rarely observed in natural rain, it may be assumed that drops larger than this usually become unstable and break up prior to reaching the ground. It has been shown that falling drops greater than 1mm in radius become distorted. The drop flattens and becomes lenticular in shape, then the base develops a concave depression and soon after develops a bubble supported by an annular ring containing the bulk of the water. The bubble

then bursts producing a fine spray of droplets, while the annular ring breaks up into several large fragments (Fig. 5).

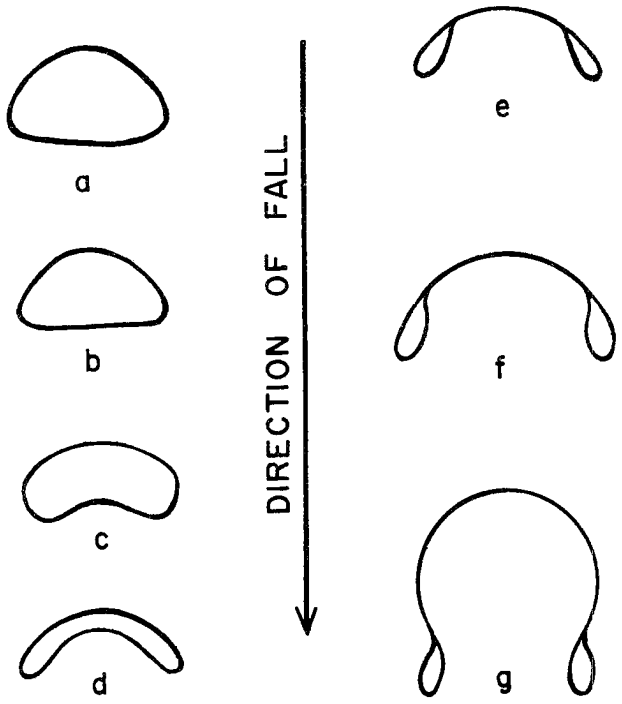

Fig. 5 A schematic representation of the stages in the disruption of a large falling drop. Adapted from Matthews and Mason, 1964.

The critical conditions for breakup were calculated by Matthews and Mason (1964). It was demonstrated that for drops of equivalent spherical radius $r < 4mm$, that the critical velocity, V_c for breakup is given by

$$V_c^2 R = 4\gamma/n\rho' C_D \tag{35}$$

where γ is the surface tension of the liquid, ρ' the air density, C_D the drag coefficient of the drop, and n a numerical factor $(1 \leq n \leq 2)$ relating the ratio of the curvature of the drop at the upper pole to its equivalent spherical radius.

A relationship of the form

$$V^2R = \text{constant}, \tag{36}$$

would be expected if it were assumed that the drop would break up when the force due to the aerodynamic pressure over the drop exceeded that due to surface tension. This compares well with the experimental expression developed by Lane (1951).

$$V_c^2R = 3.06 \times 10^5 \text{ (cgs units)} \tag{37}$$

or

$$R_c = 3.06 \times 10^5/V^2 \ . \tag{38}$$

The exact manner in which raindrops break up in a cloud may be different than that indicated by laboratory experiments; however, there is little reason to doubt that raindrops tend to break up after attaining a radius of about 2.5mm. The model utilizes (38) to determine the critical break-up radius. It is then assumed that the drops break up into four drops containing a combined volume of one half the original drop and a great number of smaller droplets. The subsequent growth of one of the larger drops is then followed.

Spengler and Gokhale (1973) investigated the role that drop impactions might have on the development of intense precipitation. They concluded that this phenomenon becomes important after a sufficient number of drops $\geq$ 2mm have been produced. They further concluded that breakup by impaction would be important only after rainfall intensities of 50mm hr^{-1} had been obtained and a major result of this breakup mechanism would be the reduction in raindrops large enough to break up due to instability. Because of the difficulty in parameterizing this process and because it contains a feedback mechanism that

reduces the effect of a droplet multiplication process already in the program, drop multiplication by impaction was neglected.

3. Loss at Cloud Top

Many of the raindrops that rise up through the cloud never return to cloud base. The top of a cumulus tower is eroded by the environmental air. In nature, this entrained air causes the liquid water content to be much lower at the leading edge of the cloud than the cloud model would indicate. Because of the low liquid water content, increased wind shear, and uncertain changes in the divergence of the rising air, the drop is assumed to be ejected from the cloud and evaporated if it comes within 50m of cloud top.

4. Duration of Rainfall

The duration of rainfall was calculated using the method developed by Weinstein and Davis (1968). In a steady state model the raindrops created at the cloud top will be the last to fall out. The duration of precipitation (D) can then be estimated as:

$$D = (z/V)_{Top} \tag{39}$$

where V is the raindrop terminal velocity at the top of the cloud.

Empirical evidence indicates that the duration calculated by this method is off by a factor of two so (39) was corrected to make calculated results agree better with observation.

$$D = 2.0(z/V)_{Top} \tag{40}$$

Because a one dimensional steady state model is not designed to give information concerning time, this calculation should be considered as an approximate order of magnitude calculation.

5. Efficiency

The efficiency of the precipitation mechanism is taken to be the ratio of precipitated water to condensed water available in the cloud. The condensed water available was calculated by two methods. The first calculated the amount in the cloud when precipitation began, the second also included water made available while precipitation was occurring. It was assumed that the condensed water was produced at the same rate in the precipitating cloud, as in the non-precipitating cloud. This results in an overestimation of water available, because of the alterations made on the updraft by the precipitation process. The true efficiency would fall in between the two calculated and, for this paper, was considered to be their mean.

TESTING THE MODEL

The Institute of Atmospheric Sciences, South Dakota School of Mines and Technology conducted Cloud Catcher, a cumulus cloud modification program, during the summer months of 1969-71. The purpose of Cloud Catcher was to determine the effect of salt and of silver iodide seeding upon convective clouds. Their results have been well documented (Koscielski and Dennis 1971, and Kosielski, Dennis, Hirsch and Biswas 1971) and provide a good data sample upon which to test the model described in the previous chapters.

A data summary for the salt seed and no seed cases is given in Tables I and II. Cloud base height and updraft radius were estimated from aircraft observations. Cloud depth and rainfall amount were determined by radar. On many days the radar determined rainfall was adjusted to take account of such items as missing data due to outages, occasional spurious signals due to noise in the radar set, and test cases moving beyond the test grid. These adjustments were subjective in nature. Experimental days of 13 July 1970, 28 July 1970, 13 August 1970, and 13 August 1971 were omitted from this study because a frontal passage occurred during the day making the 00GMT sounding unrepresentative of the air mass in which the seeding actually took place.

The mass of effective salt nuclei was actually much less than that indicated by Table II. During Project Cloud Catcher a sample of the salt used for seeding was examined to determine the particle size distribution. The results are shown in Table III. Only 9.5% of the total mass was in the range of 50μ radius or less. The larger particles are too large to be effective as seeding agents. They either do not reach

TABLE I

SUMMARY OF SEED CASES

Case	Date	Cloud Base Height (km)	Cloud Depth (km)	Updraft Radius (km)	Rainfall (acre ft)	Amount of Salt Used (lb)
1	6/06/69	3.05	6.10	1.3	50	225
2	6/06/69	3.05	6.71	1.3	200	125
3	6/25/69	2.19	5.49	1.5	50	125
4	6/30/69	3.05	1.83	0.7	2	125
5	6/30/69	3.05	1.83	0.7	0	125
6	7/07/69	Radiosonde Data Not Available				
7	7/09/69	3.60	6.40	1.3	1000	100
8	7/15/69	3.35	3.96	1.4	0	75
9	7/21/69	3.14	5.49	1.2	300	100
10	7/21/69	3.14	8.53	1.4	757	125
11	7/22/69	3.41	8.23	2.8	502	125
12	7/23/69	2.56	6.71	0.8	14	125
13	7/25/69	3.35	1.52	0.3	0	30
14	7/29/69	3.47	6.70	2.1	129	100
15	8/05/69	2.93	5.49	1.5	200	100
16	8/15/69	4.05	4.27	0.8	43	100
17	6/09/70	4.02	6.10	1.2	60	80
18	6/29/70	2.90	3.96	0.5	0	120
19	7/08/70	2.99	5.18	0.6	116	100
20	7/08/70	2.99	7.62	1.2	374	100
21	7/08/70	2.99	5.49	0.6	570	100
22	7/13/70	2.68	3.96	0.6	0	75
23	8/17/70	4.02	6.10	1.8	234	125
24	8/17/70	4.02	5.18	1.3	29	75
25	8/27/70	2.99	7.00	1.1	500	150
26	8/04/70	3.05	9.45	2.6	1200	150
27	8/05/70	2.90	10.67	2.0	465	225
28	8/05/70	2.90	10.67	2.0	1982	200
29	8/13/70	3.44	3.05	0.4	5	125
30	6/21/71	3.05	9.14	2.2	1935	125
31	6/22/71	4.08	2.43	0.5	16	350
32	7/06/71	3.84	6.71	2.5	1319	150
33	7/09/71	3.23	6.40	0.8	24	100
34	7/09/71	3.23	8.84	2.8	1289	150
35	7/09/71	3.23	6.40	0.8	1288	250
36	8/12/71	4.08	3.66	1.0	183	160
37	8/12/71	4.08	3.35	1.0	14	100
38	8/13/71	3.35	6.40	0.4	499	150
39	8/13/71	3.35	6.40	0.4	1136	200
40	8/13/71	3.35	6.40	0.4	3313	200
41	8/13/71	3.35	6.40	0.4	1057	150

TABLE II

SUMMARY OF NO SEED CASES

Case	Date	Cloud Base Height (km)	Cloud Depth (km)	Rainfall (acre ft)
1	6/06/69	3.05	3.96	0
2	6/25/69	2.20	7.01	104
3	6/07/69	2.38	3.05	0
4	7/08/69	3.35	1.52	0
5	7/08/69	3.35	4.27	3
6	7/15/69	3.35	5.79	206
7	7/17/69	2.42	7.62	160
8	7/18/69	2.41	3.96	2
9	7/22/69	3.41	4.27	115
10	7/23/69	2.56	9.75	1000
11	8/04/69	2.68	8.84	259
12	8/04/69	2.68	7.62	527
13	8/15/69	4.05	5.79	77
14	6/08/70	2.98	7.62	123
15	6/08/70	2.98	9.14	1061
16	6/08/70	2.98	9.14	1363
17	6/18/70	2.98	4.89	38
18	6/18/70	2.98	4.88	29
19	6/24/70	2.68	7.92	361
20	7/09/70	2.90	8.84	671
21	7/09/70	2.90	4.27	0
22	7/10/70	3.47	8.23	100
23	7/22/70	2.53	4.27	5
24	7/22/70	2.53	7.01	117
25	7/28/70	2.68	4.57	5
26	7/28/70	2.68	9.45	822
27	7/28/70	2.68	9.45	822
28	7/28/70	2.68	3.66	0
29	7/29/70	2.65	4.57	3
30	7/31/70	2.59	3.35	16
31	7/31/70	2.59	6.40	499
32	8/06/70	2.99	10.67	865
33	8/06/70	2.99	10.67	622
34	7/22/71	3.47	5.79	1316
35	7/22/71	3.47	4.87	271
36	7/22/71	3.47	6.40	524
37	8/03/71	3.84	2.74	1
38	8/04/71	3.38	5.79	1666

TABLE III

DISTRIBUTION OF SALT PARTICLES BY SIZE

Radius (μ)	% of Total Particles	% of Total Mass
0-5	68.0	0.01
5-10	16.7	0.4
10-15	2.8	0.3
15-20	2.1	0.5
20-25	0.8	0.4
25-30	1.3	0.7
30-35	0.5	0.7
35-40	1.1	2.3
40-45	0.3	0.8
45-50	0.8	3.4
50-55	1.9	10.6
55-60	1.3	9.8
60-65	0.3	2.5
65-70	0.3	3.2
70-75	1.1	15.5
75-80	0.5	9.6
80-85	0.5	11.6
85-90	0.0	0.0
90-95	0.5	16.2
95-100	0.0	0.0
100-105	0.3	10.8

cloud base or do not rise high enough above cloud base to be efficient as collectors of cloud water.

1. Model Verification

The numerical model listed in Appendix C was run on each of the test cases using the data in Table I and Table II for the model input of updraft radius and amount of salt used. The mass of effective nuclei was assumed to be 10% of the total mass of salt. It was further assumed that the salt particles had a uniform equivalent volume radius of 10μ, that they were homogeneously dispersed, and that the clouds were seeded at the proper time in their growth cycle. Cloud radius was assumed to be twice the updraft radius and updraft velocity at

cloud base was taken to be $2ms^{-1}$. If observed values of these parameters were available, correlation between model-predicted and observed values would probably be higher.

Correlations were made between the predicted and observed cloud bases, cloud depth, liquid-water content, updraft velocity, and rainfall. The correlation for seed and no seed cases combined was .62 for cloud base and .71 for cloud depth. Superimposed data were not plotted for clarity of the figures.

The mean predicted cloud base was 3.38 km and the mean observed cloud base was 3.21 km. This difference is partially accounted for by the location of Rapid City. On days with easterly winds the Black Hills act as a barrier causing forced lifting of the air. On these days formation of cloud bases follow more accurately a lifted rather than a convective process. This results in lower cloud bases.

A small data sample of liquid water content and updraft velocity observed by instrumented aircraft was available. These were compared with the values predicted by the model at the level of aircraft penetration, which was generally about 3.0 km above cloud base. It was assumed that the largest values obtained during a penetration were representative of the updraft core. The mean observed liquid-water content was 4.2 compared to 4.5 gm^{-3} predicted by the model. The worst data fits for liquid-water content are values over predicted, by as much as a factor of two. It is possible that on these occasions the aircraft did not penetrate the core of the rising air mass and missed the area of maximum liquid-water content.

The observed versus predicted rainfall for all seeded cases is shown in Figure 12. When all cases in which ice was observed in the

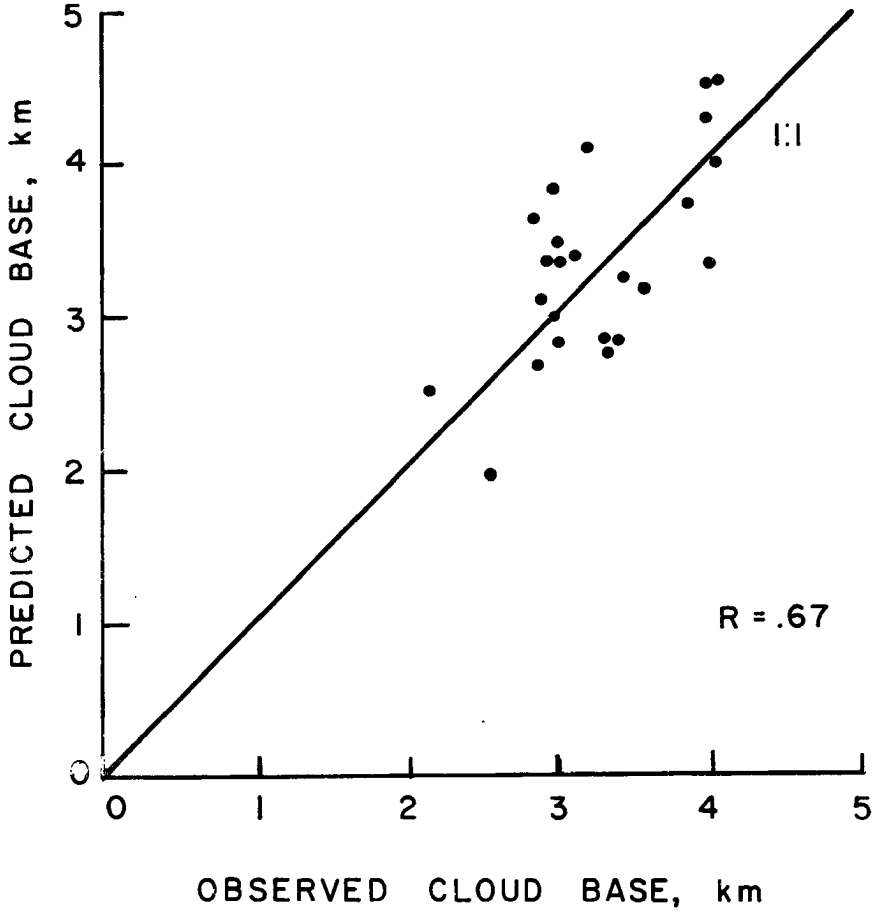

Fig. 6 Observed versus model-predicted cloud base, for seed cases.

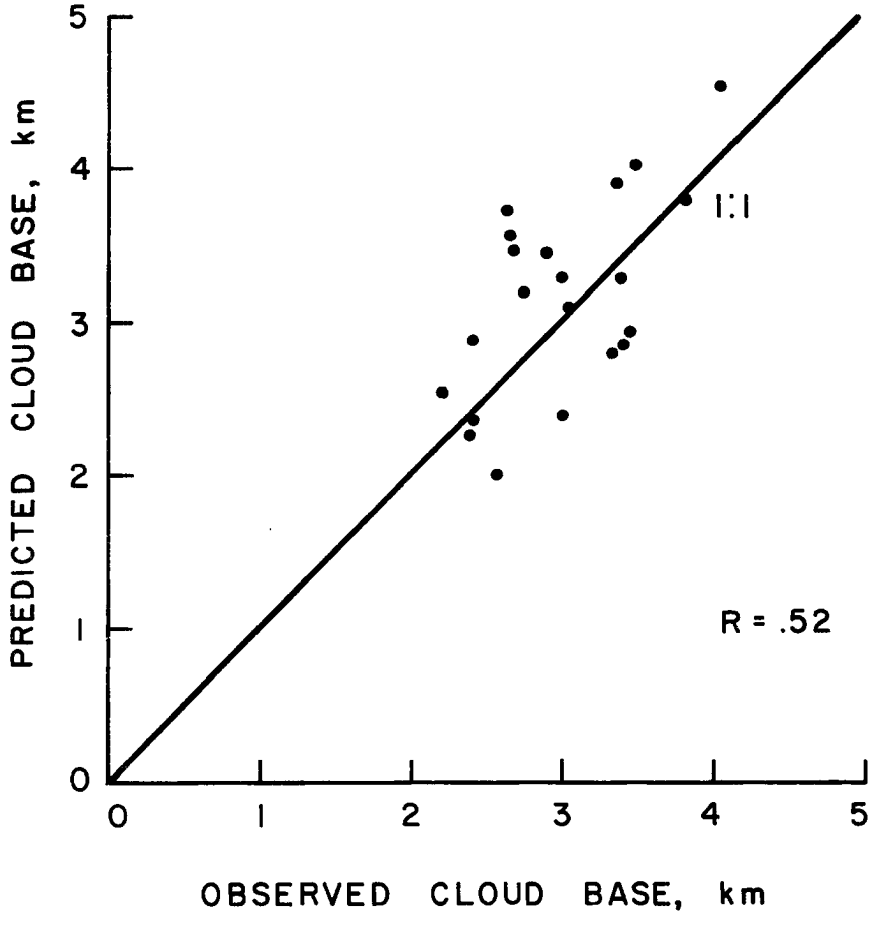

Fig. 7 Observed versus model-predicted cloud bases, for no-seed cases.

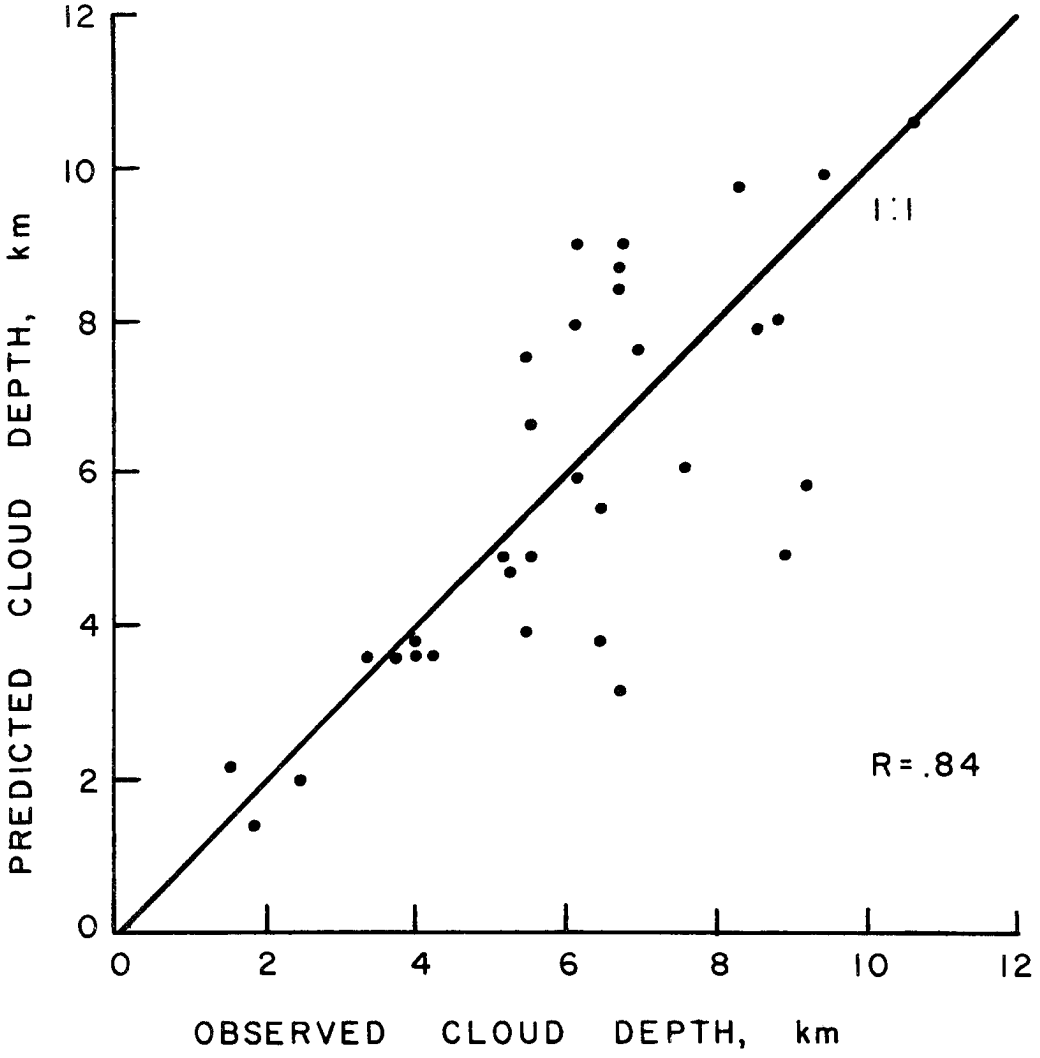

Fig. 8 Observed versus model-predicted cloud depth, for seed cases.

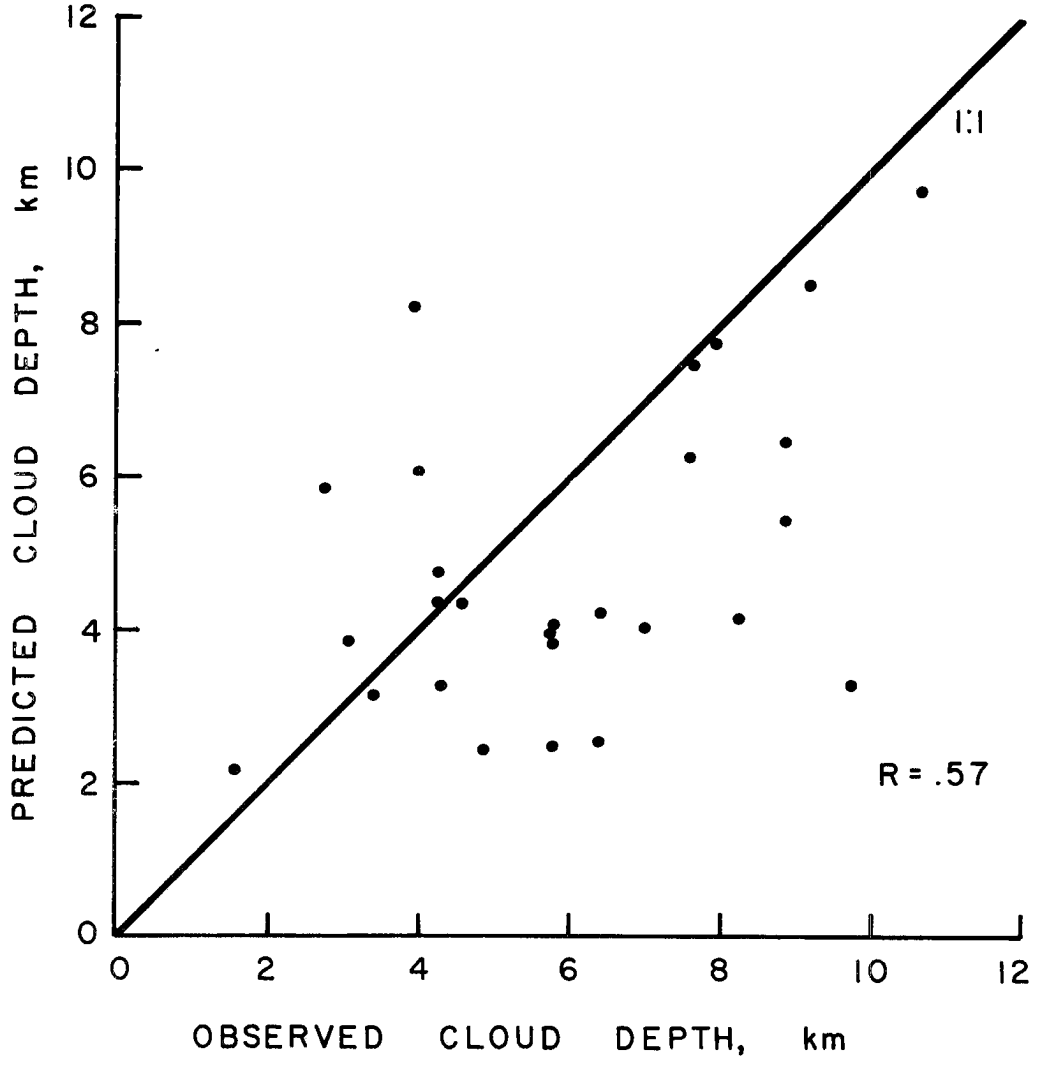

Fig. 9 Observed versus model-predicted cloud depth for no-seed cases.

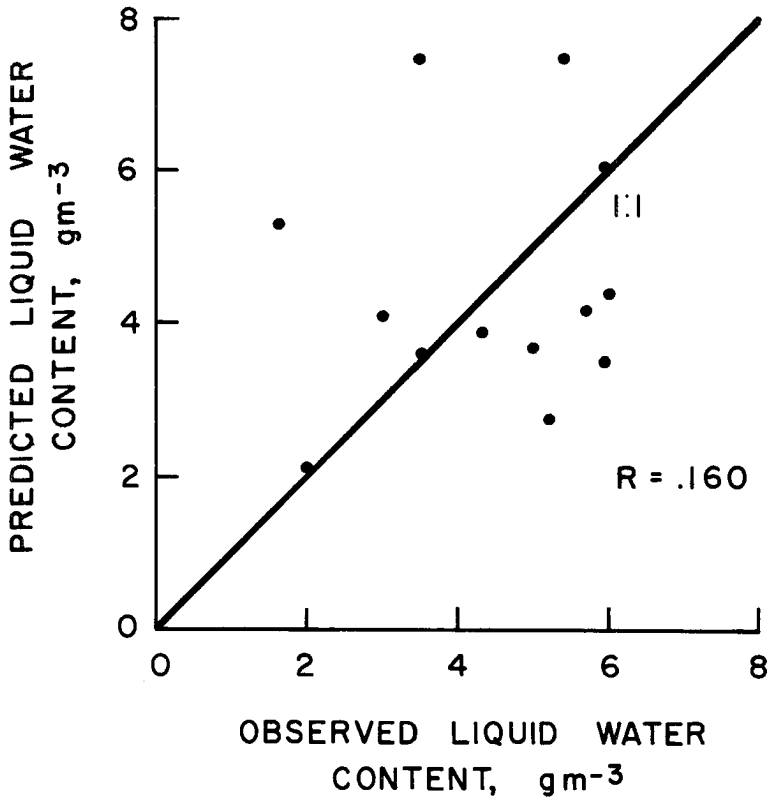

Fig. 10 Observed versus model-predicted liquid-water content.

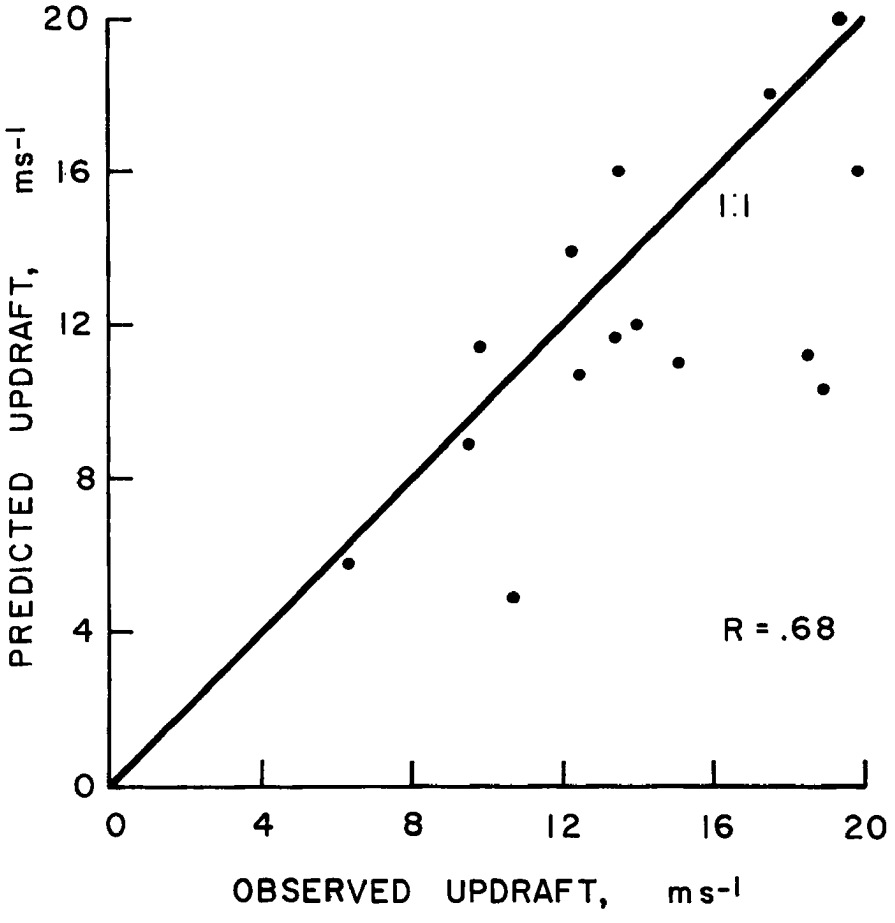

Fig. 11 Observed versus model-predicted updraft velocity.

cloud prior to seeding were removed from the data sample, the correlation improves from .49 to .81. (Fig. 13) The cases in which ice was not observed prior to precipitation were more likely to have the rainfall caused by a coalescence process induced by the salt seeding. While salt seeding may have influenced the precipitation in the "ice" clouds, it is likely that the dominate precipitation mechanism was an ice process.

The model results indicated that the warm rain processes play a minor role in the natural development of precipitation in the Rapid City area. For the no-seed cases the model predicted that precipitation could form through coalescence only for the two cases occurring on 6 August 1970. The results for the predicted versus observed rainfall amounts for the no-ice days are shown in Table IV.

TABLE IV

SUMMARY OF MODEL PREDICTED AND OBSERVED RAINFALL FOR NO-SEED CASES IN WHICH THE WARM PRECIPITATION MECHANISM APPEARED DOMINANT

Case #	1	3	4	8	21	29	30
Predicted Rainfall (acre-ft)	0	0	0	0	0	0	0
Observed Rainfall (acre-ft)	0	0	0	2	0	3	16

A summary of correlation coefficients found by previous investigators using various numerical models is given in Table VII. There are two explanations for the smaller correlations of the model under investigation. The previous studies used observed rather than calculated cloud bases as input to the model. Any variation in cloud base

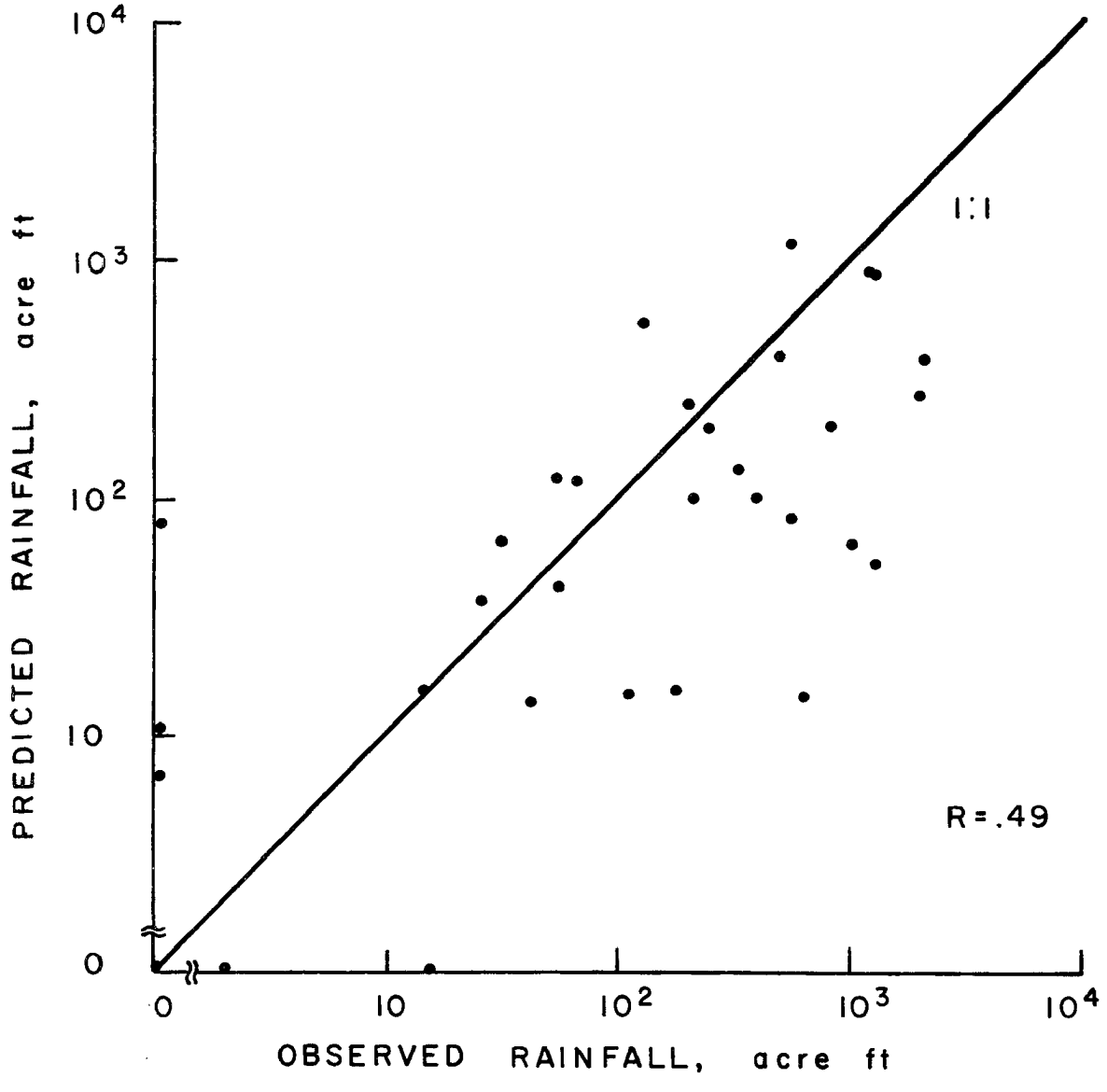

Fig. 12 Observed versus predicted rainfall amounts, for all cases.

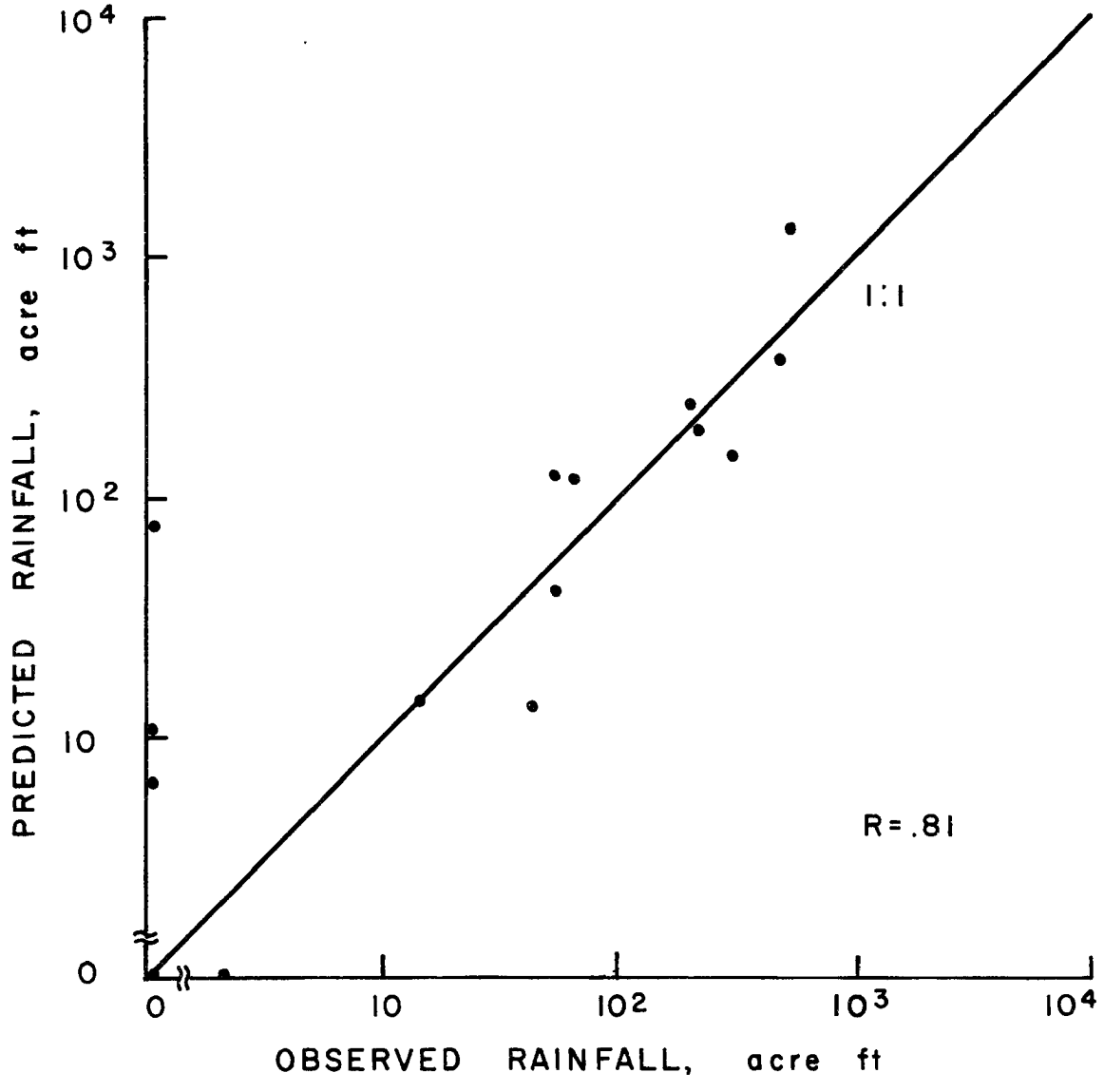

Fig. 13 Observed versus predicted rainfall amounts for those clouds in which the warm precipitation mechanism was dominant.

TABLE V

SUMMARY OF PREDICTED VERSUS OBSERVED DATA FOR SEED CASES

Case	Seed						
	Cloud Base (km)		Cloud Depth		Rainfall (acre-ft)		Type* Day
	Predicted	Observed	Predicted	Observed	Predicted	Observed	
1	3.06	3.05	8.99	6.10	123	50	1
2	3.06	3.05	8.99	6.71	107	200	2
3	2.56	2.19	3.92	5.49	43	50	1
4	2.84	3.05	1.43	1.83	0	2	1
5	2.84	3.05	1.43	1.83	0	0	1
6	Radiosonde Data Not Available						2
7	3.21	3.60	3.83	6.40	60	1000	2
8	2.79	3.35	3.67	3.96	68	0	1
9	3.39	3.14	7.53	5.49	140	300	1
10	3.39	3.14	7.88	8.53	205	757	2
11	2.83	3.41	9.69	8.23	1211	502	1
12	1.99	2.56	3.10	6.71	16	14	1
13	2.87	3.35	2.13	1.52	6	0	1
14	3.27	3.47	8.69	6.70	504	129	2
15	3.13	2.93	6.58	5.49	253	200	1
16	4.53	4.05	3.63	4.27	15	43	1
17	3.36	4.02	7.88	6.10	118	60	1
18	3.64	2.90	3.79	3.96	11	0	1
19	3.82	2.99	4.96	5.18	16	116	2
20	3.82	2.99	6.21	7.62	97	374	2
21	3.82	2.99	4.96	5.49	16	570	2
22	3.72	2.68	1.87	3.96	3	0	3
23	4.32	4.02	6.01	6.10	197	234	1
24	4.32	4.02	4.73	5.18	63	29	2
25	3.43	2.99	7.61	7.00	77	500	2
26	3.41	3.05	9.87	9.45	828	1200	2
27	2.72	2.90	10.67	10.67	379	465	1
28	2.72	2.90	10.67	10.67	378	1982	2
29	5.01	3.44	1.97	3.05	0	5	3
30	3.53	3.05	5.82	9.14	276	1935	**
31	4.03	4.08	1.94	2.43	0	16	
32	3.76	3.84	8.43	6.71	801	1319	
33	4.13	3.23	5.56	6.40	36	24	
34	4.13	3.23	8.01	8.84	796	1289	
35	4.13	3.23	5.56	6.40	48	1288	
36	4.56	4.08	3.65	3.66	15	183	

TABLE V (cont'd)

SUMMARY OF PREDICTED VERSUS OBSERVED DATA FOR SEED CASES

	Seed						
	Cloud Base (km)		Cloud Depth		Rainfall (acre-ft)		Type*
Case	Predicted	Observed	Predicted	Observed	Predicted	Observed	Day
37	4.56	4.08	3.65	3.35	16	14	
38	4.21	3.35	2.49	6.40	NA	499	3
39	4.21	3.35	2.49	6.40	NA	1136	3
40	4.21	3.35	2.49	6.40	NA	3313	3
41	4.21	3.35	2.49	6.40	NA	1057	3

*1. No ice in cloud visible prior to seeding

2. Ice in cloud visible prior to seeding or cloud observation not possible (eg. due to obscurring lower clouds)

3. Frontal passage causes 00GMT sounding to be unrepresentative

**Cloud observations were not available for 1971 cases

TABLE VI

SUMMARY OF PREDICTED VERSUS OBSERVED DATA FOR NO SEED CASES

	No Seed						
	Cloud Base		Cloud Depth		Rainfall		
Case	Predicted	Observed	Predicted	Observed	Predicted	Observed (acre ft)	Type
1	3.06	3.05	8.23	3.96	No	0	1
2	2.56	2.20	4.06	7.01	No	104	2
3	2.88	2.38	3.84	3.05	No	0	1
4	3.30	3.35	2.22	1.52	No	0	1
5	3.30	3.35	4.36	4.27	No	3	2
6	2.79	3.35	4.04	5.79	No	206	2
7	2.41	2.42	-	7.62	No	160	4
8	2.32	2.41	6.08	3.96	No	2	1
9	2.83	3.41	4.76	4.27	No	115	2
10	1.99	2.56	3.32	9.75	No	1000	2
11	3.49	2.68	6.49	8.84	No	259	2
12	3.49	2.68	6.30	7.62	No	527	2
13	4.53	4.05	3.99	5.79	No	77	2
14	3.31	2.98	7.51	7.62	No	123	2
15	3.31	2.98	8.55	9.14	No	1061	2
16	3.31	2.98	8.55	9.14	No	1363	2
17	2.41	2.98	-	4.88	No	38	4
18	2.41	2.98	-	4.88	No	29	4
19	3.19	2.68	7.80	7.92	No	361	2
20	3.47	2.90	5.43	8.84	No	671	2
21	3.47	2.90	3.29	4.27	No	0	1
22	2.95	3.47	4.18	8.23	No	100	2
23	3.62	2.53	4.71	4.27	No	5	3
24	3.62	2.53	5.18	7.01	No	117	3
25	4.26	2.68	3.06	4.57	No	5	3
26	4.26	2.68	4.84	9.45	No	822	3
27	4.26	2.68	4.84	9.45	No	822	3
28	4.26	2.68	2.50	3.66	No	0	3
29	3.54	2.65	4.35	4.57	No	3	1
30	3.72	2.59	3.15	3.35	No	16	1
31	3.72	2.59	4.26	6.40	No	499	2
32	2.38	2.99	9.76	10.67	Yes	865	2
33	2.38	2.99	9.76	10.67	Yes	622	2
34	4.03	3.47	2.52	5.79	No	1316	**
35	4.03	3.47	2.47	4.87	No	271	
36	4.03	3.47	2.57	6.40	No	524	
37	3.81	3.84	5.85	2.74	No	1	
38	3.92	3.38	3.88	5.79	No	1666	

1 No ice in cloud prior to precipitation

2 Ice in cloud prior to precipitation or cloud observation not possible (eg. cloud obscurred by lower clouds)

3 Frontal passage causes 0000T sounding to be unrepresentative

4 Air mass too stable to allow cloud formation at determined cloud base

**Cloud observations not available for 1971 cases

causes a change in the total energy available to the cloud from condensation, resulting in errors in the prediction of cloud depth and precipitation amounts.

TABLE VII

SUMMARY OF CORRELATION COEFFICIENTS BETWEEN MODEL-PREDICTED AND OBSERVED PARAMETERS

Parameter	Correlation Coefficient	Location of Investigation	Principal Investigator
Cloud-Top Height	0.92	Caribbean Sea	Sax (1967)
Cloud-Top Height	0.88	Pennsylvania	Davis (1967)
Cloud-Top Height	0.88	Arizona	MRI (1968)
Rainfall Amount	0.89	Arizona	MRI (1968)
Cloud-Top Height	0.82	South Dakota	Hirsch (1971)
Vertical Velocities	0.61	South Dakota	Hirsch (1971)
Liquid-Water Content	0.30	South Dakota	Hirsch (1971)
Cloud-Base	0.62	South Dakota	Durham
Cloud-Depth	0.71	South Dakota	Durham
Rainfall Amount	0.81	South Dakota	Durham
Liquid-Water Content	0.16	South Dakota	Durham
Vertical-Velocities	0.68	South Dakota	Durham

The second explanation is that the vertical profile provided by the radiosonde was not representative of the air actually entrained into the cloud. Soundings were taken at the Rapid City Regional Airport, often several hours after the test case data was taken. The greatest deviation between observed and predicted values were for clouds with updraft radii smaller than 1 km. A small error in the updraft radius could cause a significant change in the entrainment rate in these small clouds.

2. Sensitivity Analysis

A sensitivity analysis was made to indicate where possible errors are most significant. The input parameters of updraft velocity, droplet concentration, and droplet size were varied by 50%, and the cloud base height was varied by 500 m from the calculated value to test their effect on the model predicted values of cloud depth, maximum updraft, velocity, maximum liquid-water content and precipitation. The model was run using the average Rapid City July sounding as input for the vertical profile of the atmosphere. The comparisons were made against the values predicted by the model using as input an updraft velocity of $2ms^{-1}$, droplet concentration of $350cm^{-3}$, and average droplet radius of 3.5μ. The most sensitive parameters were the cloud base height and the initial updraft velocity. Observed data can be used for these terms during field operations. This could significantly increase the accuracy of the models predictions.

3. Summary

A simple model of the warm phase precipitation process in a steady-state cumulus cloud has been described and tested. It utilized versions of the first law of thermodynamics and the third law of motion along with modified continuous growth equations that describe precipitation development.

The main limitations of the model are:

1. The model ignores the diffusion of the salt particles within the cloud.
2. The model neglects horizontal asymmetries.
3. Initial conditions at cloud base are required as input.
4. Continuous growth equations are used in lieu of the more accurate stochastic equations.

TABLE VIII

SUMMARY OF PREDICTED PARAMETERS UNDER VARIOUS CONDITIONS

Initial Updraft Velocity (cms^{-1})	Cloud Depth (km)	Precipitation (acre-ft)	Max Vertical Velocity (ms^{-1})	Max Liquid-Water Content (gm^{-3})
200	4.9	58.9	12.8	5.0
100	4.6(-6.0)*	52.5(-11.0)	11.7(-9.0)	5.0(0)
300	5.1(+4.0)	62.7(+6.0)	13.6(+6.0)	5.0(0)
Droplet Concentration ($\#cm^{-3}$)				
350	4.9	58.9	12.8	5.0
175	4.9	57.9(-2.0)	12.8(0)	5.0(0)
525	4.9	58.8(+0.0)	12.8(0)	5.0(0)
Average Initial Droplet Size (μ) (No Seed)				
3.5	4.9	0	12.8	5.0
2.0	4.9	0(0)	12.8(0)	5.0(0)
7.0	4.9	0(0)	12.8(0)	5.0(0)
Cloud Base (km) (MSL)				
3.15	4.9	58.9	12.8	5.0
2.65	5.7(+6.0)	73.6(+25.0)	15.2(+19.0)	6.2(+24.0)
3.65	4.1(-16.0)	42.0(-29.0)	10.7(-16.0)	4.1(-18.0)

*Denotes percentage change

Testing of the model indicated a fair correlation between predicted and observed values of cloud base and cloud depth. The correlation with observed rainfall was good for cases in which there was a fair degree of certainty that the warm precipitation process was dominant. The accuracy of the model decreased for clouds with small updraft radii. The model was most sensitive to input values of cloud base height and initial updraft velocity.

APPLICATION OF THE MODEL

The model has been shown to work reasonably well for clouds in the Rapid City area. Extrapolation of the results of this test to other areas of the Great Plains must be done with care. Predictions from one-dimensional steady-state models are very sensitive to cloud base height. This sensitivity is greatest in the south-eastern portions of the Great Plains. In this area cloud bases are often low, and the saturated mixing ratio decreases rapidly with height. An error of 500 m in cloud base height can cause significant errors in the total energy available to the cloud from condensation, and a similar error in the estimate of rainfall from the cloud. While there is no reason to believe that the results of the model verification would have been significantly different had the data come from another area of the Great Plains, it is doubtful that they would have been duplicated.

The model was run on the average July soundings for Rapid City, South Dakota; Denver, Colorado; Fort Worth, Texas and Columbia, Missouri to determine the relative effectiveness of the natural coalescence process, the optimum size of sodium chloride for use in seeding and the optimum seeding density for each station. These results were then used to calculate the potential for hygroscopic seeding in the various areas of the Great Plains.

1. Natural Coalescence Process

The numerical model showed that the warm precipitation mechanism plays an important role in the development of rain in the southern region of the Great Plains. Rainfall was predicted to develop in non-seeded clouds of 3.0km radius, on more than 20% of the days in the

Fort Worth and Columbia areas, and on less than 2% of the days in the Denver and Rapid City areas (Table IX).

TABLE IX

SUMMARY OF NUMBER OF DAYS ON WHICH THE MODEL PREDICTED THE DEVELOPMENT OF PRECIPITATION THROUGH A NATURAL COALESCENCE PROCESS

Cloud Radius (km)	1.0	2.0	3.0
Columbia	2(1.2)*	16(9.7)	33(21.3)
Denver	0	0	0
Fort Worth	0	1(0.6)	38(24.5)
Rapid City	0	0	3(2.0)

*Denotes percentage

The lack of importance of the warm coalescence process in the more continental areas of the Great Plains is primarily due to the higher droplet concentrations and lower liquid-water contents of the clouds in these regions. Both of these conditions tend to suppress the coalescence process.

2. Optimum Size and Seeding Density

The optimum size for sodium chloride seeding agents was found by using various sizes as input to the numerical model to determine which size swept out the most water. On the average sounding this was always the particle that came closest to the top of the cloud without being ejected (Fig. 14). The most rapid growth rate of the drop takes place during their fall to cloud base. Solution drops formed from the large salt particles grow too rapidly. They become large enough to fall against the updraft at a relatively low level in the cloud and sweep out very little water during their fall to cloud base.

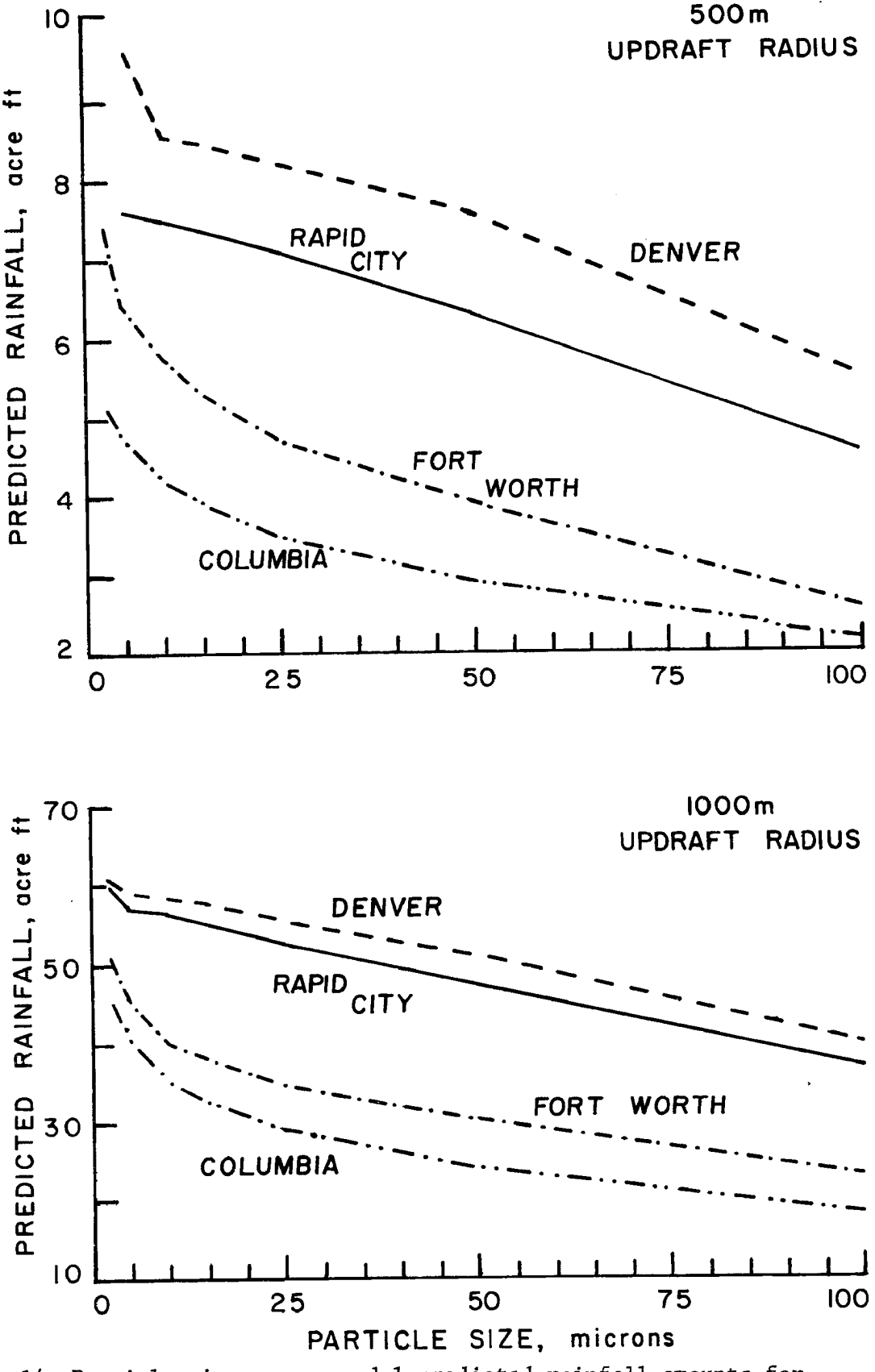

Fig. 14 Particle size versus model-predicted rainfall amounts for various updraft radii and different areas of the Great Plains.

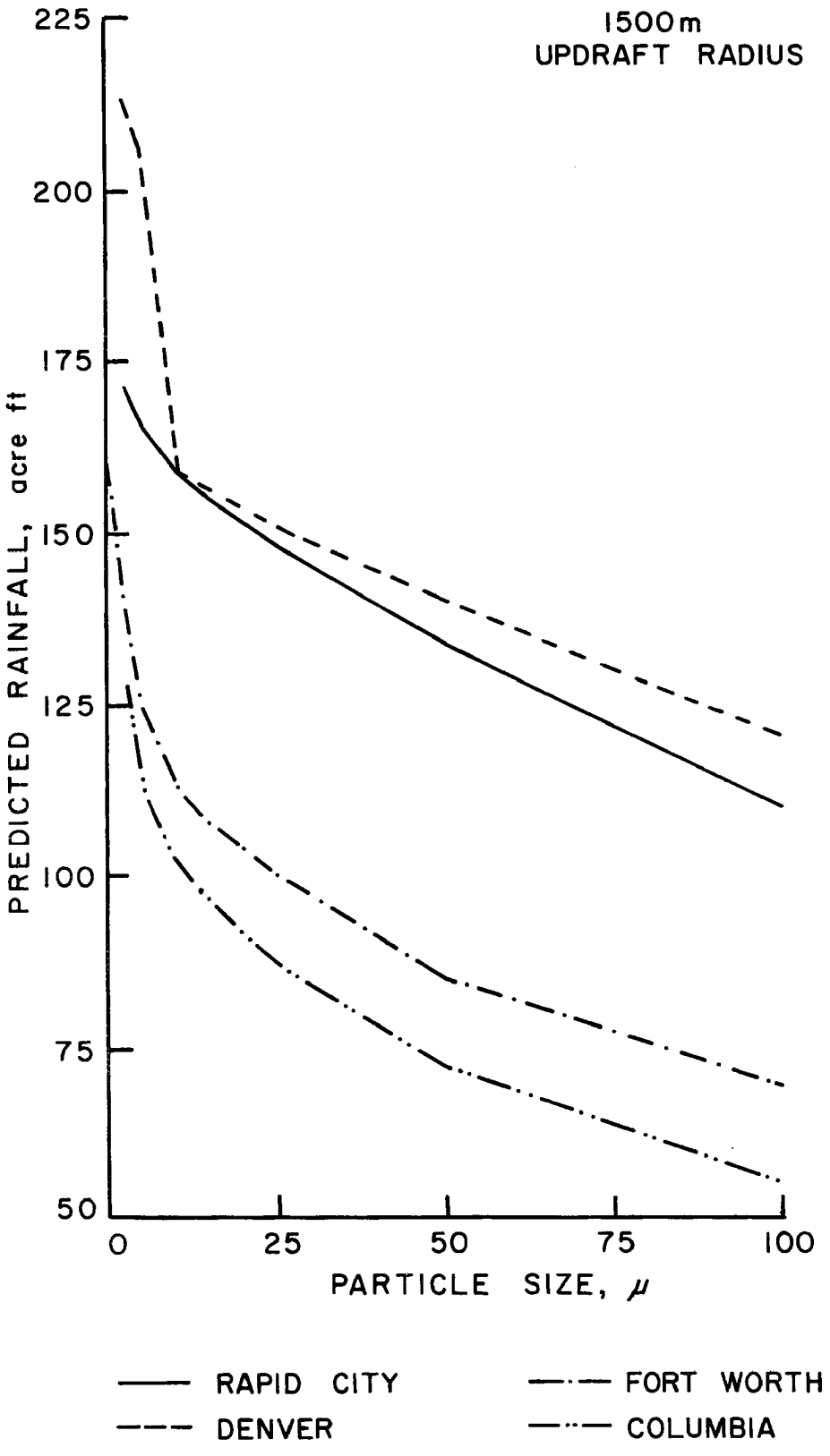

Fig. 14 (cont'd) Particle size versus model-predicted rainfall amounts for various updraft radii and different areas of the Great Plains.

The small particles have a much longer trajectory through the cloud and can reach the critical size for breakup.

When the optimum seeding size calculated using the averaged soundings was run on a daily basis, a large number of clouds did not precipitate. Because of this the optimum seeding size was increased by one size interval over that indicated by the average sounding. Although the smaller salt particles produced more precipitation when it did rain, this was more than compensated for by the increased number of clouds that produced precipitation using the larger size particle.

The optimum seeding density was found in a similar manner. Various seeding densities (the number of salt particles per liter at cloud base) were run in the numerical model using the optimum size salt particles. The results are shown in Figure 15. The gaps in the data are caused when one seeding density allows the drop to grow large enough to reach critical size and breakup. At higher seeding densities the added weight of the large drops decreases the buoyancy and the drops do not rise as far in the cloud and no breakup occurs. When seeding densities are increased above 100 per liter, competitition for the liquid-water reduces the growth rate and inhibits the formation of precipitation. Massive seeding with small salt particles ($R < 2.5\mu$) will create a droplet spectrum consisting of many small droplets. This will inhibit coalescence and suppress the warm precipitation process.

The optimum seeding size and density for the various cities is given in Table X.

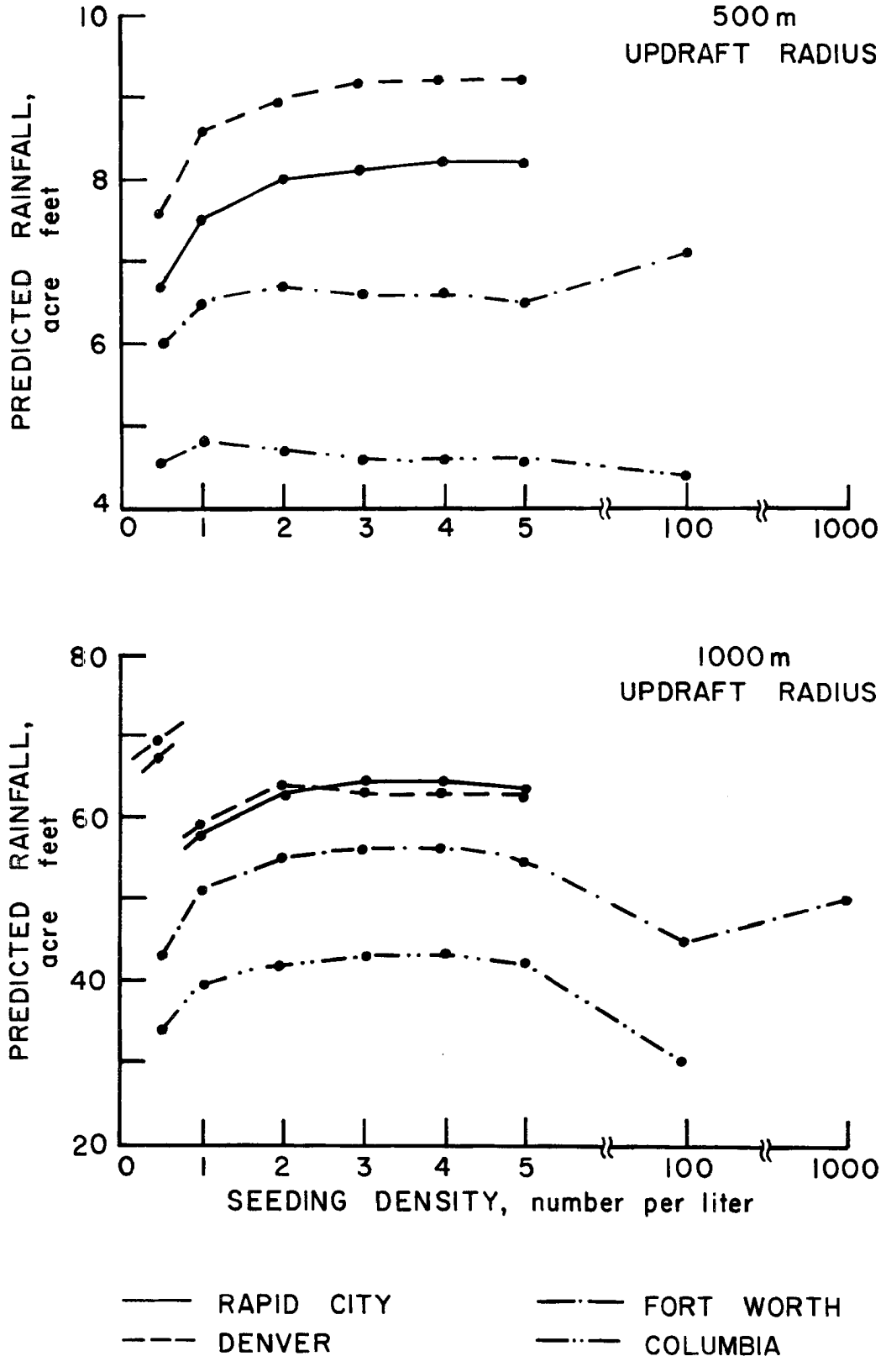

Fig. 15 Seeding density versus model-predicted rainfall amounts for various updraft radii and different areas of the Great Plains.

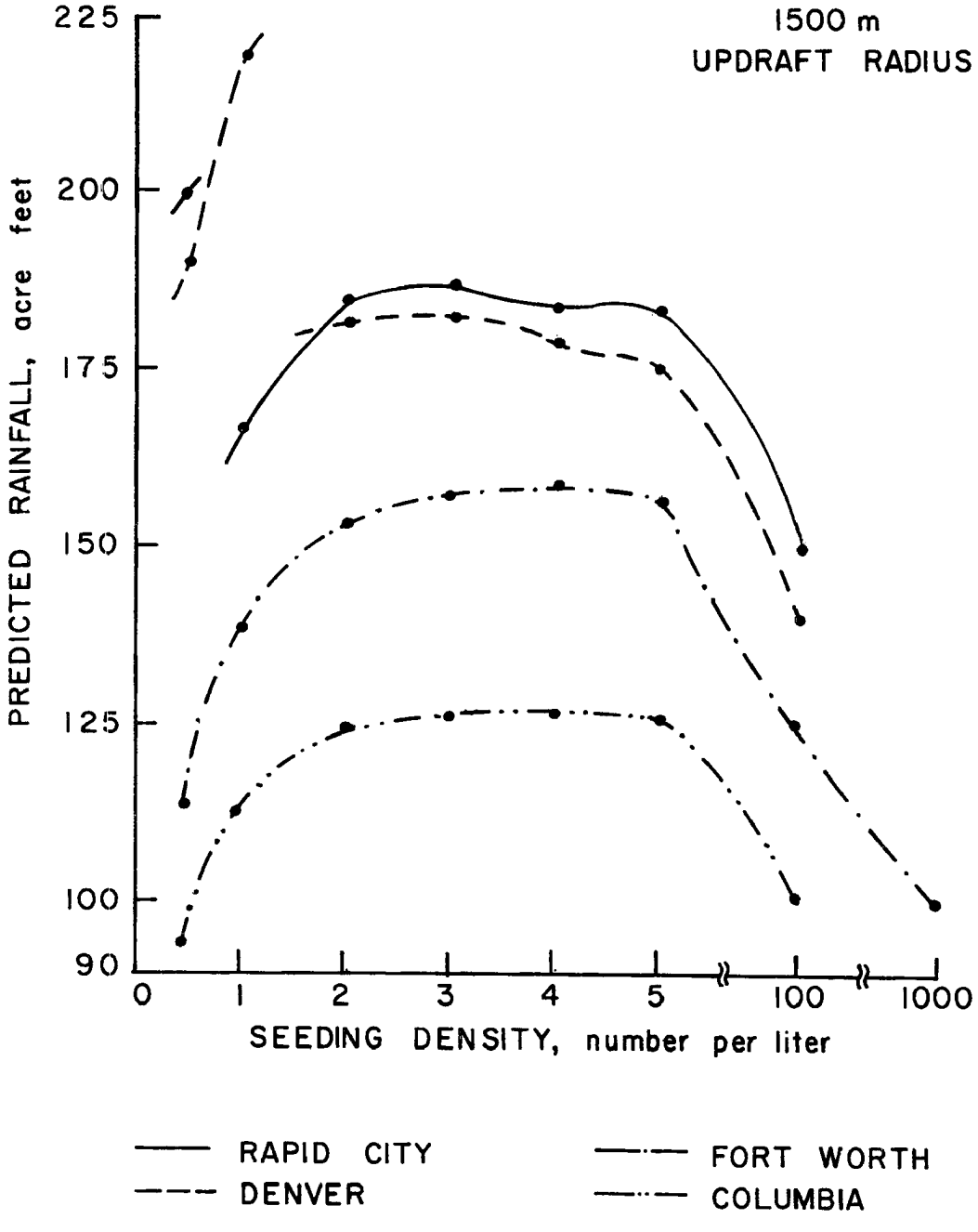

Fig. 15 (cont'd) Seeding density versus model-predicted rainfall amounts for various updraft radii and different areas of the Great Plains.

TABLE X

SUMMARY OF OPTIMUM SEEDING SIZES AND DENSITIES

	Columbia		
Updraft Radius (m)	500	1000	1500
Size(μ)	5.0	5.0	5.0
Density (#/liter)	1.0	3.0	4.0
	Denver		
Updraft Radius (m)	500	1000	1500
Size(μ)	10.0	5.0	5.0
Density (#/liter)	3.0	0.5	1.0
	Fort Worth		
Updraft Radius (m)	500	1000	1500
Size(μ)	5.0	2.5	2.5
Density (#/liter)	2.0	3.0	4.0
	Rapid City		
Updraft Radius (m)	500	1000	1500
Size(μ)	10.0	5.0	5.0
Density (#/liter)	4.0	0.5	0.5

3. Potential for Precipitation Augmentation

Using the optimum seeding sizes and densities shown in Table X the numerical model was run on the daily 00GMT soundings of the various stations. The July soundings of 1964 through 1969 were used, providing a data sample of 155 days for each station. The practical application of the results of the study, one must accept the existence of a population of clouds with a set range of horizontal dimensions. For this study the horizontal dimensions were 1000M, 2000M, and 3000M. The updraft radius was assumed to be one half the cloud radius. It was further assumed that at the time of seeding the salt particles were homogeneously dispersed through the lower 600m of the cloud. This could be accomplished by seeding for five minutes beneath a cloud with an updraft of $2ms^{-1}$. The results are shown in Table XI.

Table XI indicates that precipitation can be induced in all areas of the Great Plains through sodium chloride seeding. The greatest rainfall amounts are from the clouds in the Rapid City area. A study of the cloud top temperatures indicates that the larger clouds in the Rapid City and Denver area would have likely produced precipitation through an ice process, and may be suitable for silver iodide seeding. An area of obvious potential benefit from hygroscopic seeding is the southern Great Plains, where the seeding agents have a long trajectory through the cloud prior to reaching the freezing level. In this area many clouds that yield rainfall amounts greater than 100 acre-ft when seeded with hygroscopic particles, are unsuitable for other forms of seeding. The model shows that rainfall can develop on many days in the southern Great Plains region without seeding. On these days salt seeding could still prove beneficial by increasing the

TABLE XI

AVERAGE DAILY MODEL-PREDICTED SEEDING RESULTS

Cloud Radius (km)	Rainfall(acre-ft)	Efficiency(%)	Average Cloud Top Temperature(^{o}C)
	Columbia		
1.0	7.5	1.00	+1
2.0	54.0	2.11	-8
3.0	150.0	2.76	-17
	Denver		
1.0	7.4	1.29	-13
2.0	49.0	2.03	-21
3.0	137.0	2.80	-38
	Fort Worth		
1.0	7.0	1.00	-4
2.0	54.6	1.61	-16
3.0	147.0	2.12	-24
	Rapid City		
1.0	8.0	1.23	-8
2.0	56.5	1.95	-21
3.0	156.0	2.68	-32

number of relatively large drops, which will increase the efficiency of the precipitation process.

Because the model does not include an ice process or have the ability to evaluate the potential of silver iodide seeding, no definite statement can be made as to the relative value of hygroscopic seeding in the various areas of the Great Plains.

The Cloud Catcher program conducted in the Rapid City area showed little change in the precipitation from large cumulus clouds due to

salt seeding. This may be due in part to the amount of salt used. The large clouds received no more salt than the small clouds. The numerical model indicates that the Langmuir chain reaction is not generally effective enough to compensate for the relatively smaller amount of salt. If the seeding amount were increased with the updraft radius it is likely that a significant increase in rainfall will be found.

CONCLUSION

A one-dimensional steady-state cumulus cloud model was developed to investigate the warm precipitation mechanism in cumulus clouds. The numerical model was tested using data from an extensive field program in cumulus research conducted near the Black Hills of South Dakota. Testing of the model was done using model-predicted, rather than observed cloud bases. Good correlation coefficients were found for precipitation, cloud depth and updraft velocities when model-predicted values were compared to the aircraft observed values.

The numerical model was used to find the optimum salt particle size and seeding density in various areas of the Great Plains. It was found that the optimum particle size decreased with an increase in cloud size and increased with the continentality of the region. There was no evidence that the natural coalescence process was of major importance in cumulus clouds in the northern Great Plains. In the southeastern areas, where the cloud bases are low and moisture is much more abundant, the numerical model showed that precipitation can develop through a natural warm process.

The optimum seeding density was generally greatest in the dryer continental areas. In these areas the updrafts in clouds with the same horizontal dimensions are higher because of the smaller loss of acceleration caused by the weight of the cloud water. This allows a greater mass of raindrops to be carried upward. The effect of over seeding was highly parameterized in the model so that the results in this area are highly qualitative. Over seeding did tend to inhibit the production of rain because greater competition for the liquid-water. This was most pronounced in the more continental areas.

The final application of the model was to test the climatological potential for rainfall augmentation through sodium chloride seeding. The model showed that precipitation could be induced through salt seeding in all areas of the Great Plains. Large amounts of rainfall can be produced from clouds in south-eastern portions of the Great Plains that do extend far enough above the freezing level to be suitable for silver iodide seeding. Because the model does not allow for droplet growth by an ice process, a determination of the relative potential of salt versus silver iodide seeding could not be made.

REFERENCES

Berry, E.X., 1967: Cloud Droplet Growth by Collection. Desert Research Inst., University of Nevada, Reno, Nevada.

Betts, A.K. and Dugan, Frank J., 1973: Empirical Formula for Saturation Pseudoadiabats and Saturation Equivalent Potential Temperature. To be published June J. Appl. Meteor.

Bowen, E.G., 1950: The Formation of Rain by Coalescence. Australian Journal Science Research A, 3, 193.

Fletcher, N.H., 1966: The Physics of Rainclouds. Cambridge University Press, London, pp. 390.

Fonda, A. and Herne, H., 1957: The Aerodynamic Capture of Particles by Spheres. National Coal Board Min. Res. Rep #2068, pp. 572-573.

Foote and DuToit, 1969: Terminal Velocity of Raindrops Aloft. Journal of Applied Meteorology, 8, pp. 249-253.

Gunn, R. and Kinzer, G.D., 1949: The Terminal Velocity of Fall for Water Droplets in Stagnant Air. Journal Meteorology 6, pp. 243-248.

Hirsch, John H., 1971: Computer Modeling of Cumulus Clouds During Project Cloud Catcher, Report 71-7, Institute of Atmospheric Sciences, South Dakota School of Mines and Technology, Rapid City, South Dakota, 61 pp.

Klazura, Gerard, 1971: Measurements of Precipitation Particles in Warm Cumuli over Southeast Texas. Journal of Applied Meteorology, 10, pp. 739-750.

Klett, J.D. and Davis, M.H., 1973: Theoretical Collision Efficiencies of Cloud Droplets at Small Reynolds Numbers. Journal of Atmospheric Science, Vol. 30, pp. 107-117.

Koscielski, A., A.S. Dennis, J.H. Hirsch, and K.R. Biswas, 1971: Randomized Seeding of Convective Clouds in a Moving Target Area, Report 71-6, Institute of Atmospheric Sciences, South Dakota School of Mines and Technology, Rapid City, South Dakota, 213 pp.

Lane, W.R., 1951: Shatter of Drops in Streams of Air. Ind. Engng. Chem ind. Edn; 43, p. 1312.

Malkus, J.S., Recent Advances in the Study of Convective Clouds and Their Interaction with the Environment. Tellus, Vol. 4, pp. 71-87.

Mason, B.J., 1971: The Physics of Clouds. Clarendon Press, Oxford, pp. 671.

Matthews, J.B. and Mason, B.J., 1964: Rupture of Water Drops in an Electric Field. Quarterly Journal of the Royal Meteorological Society, 90, pp. 275-285.

Meteorology Research Inc., 1968: Arizona Weather Modification Research Program, Research Reports for FY 1968, USBR 14-06-D5589, Altadena, California, 153 pp.

Namias, J., 1939: On the Dissipation of Tall Cumulus Clouds. Monthly Weather Review, Vol. 67, pp. 294-296.

Sax, R.I., 1967: Natural and Artificial Glaciation of Tropical Cumuli. M.S. Thesis Pennsylvania State University, University Park, Pennsylvania, 85 pp.

Schock, M.R., 1968: Analysis of a Randomized Salt Seeding Experiment on Cumulus Clouds, Report 68-8, Institute of Atmospheric Sciences, South Dakota School of Mines and Technology, Rapid City, South Dakota, 39 pp.

Shafrir, V. and Neiburger, M., 1963: Collision Efficiencies of Two Spheres Falling in a Viscous Medium. Journal of Geophysical Research, 68, pp. 4141.

Simpson, J.R. and V. Wiggert, 1969: Models of Precipitating Cumulus Towers. Monthly Weather Review, 97, pp. 471-489.

Spengler, John D. and Gokhale, Narayan R., 1973: Drop Impactions. Journal of Applied Meteorology, 10, pp. 739-750.

Squires, P., 1952: The Growth of Cloud Droplets by Condensation. Australian Journal of Science Research A., 5, pp. 59-86.

Squires, P. and Turner, J.S., 1962: An Entraining Jet Model for Cumulonibus Updrafts. Tellus, Vol. 14; pp. 422-434.

Stommel, H., 1947: Entrainment of Air Into a Cumulus Cloud. Journal of Meteorology, 4, pp. 91-94.

Telford, J., 1955: A New Aspect of Coalescence Theory. Journal of Meteorology, 12, pp. 436.

Turner, J.S., 1963: The Motion of Buoyant Elements in Turbulent Surroundings. Journal of Fluid Mechanics, 16, pp. 1-16.

Weinstein, A.I. and Davis, L.G., 1968: A Parameterized Numerical Model of Cumulus Convection. Report #11 to the NSF, NSF GA-777.

APPENDIXES

APPENDIX A

LIST OF SYMBOLS

A = updraft radius

B = seeding density

C_D = drag coefficient

C_p = specific heat at constant pressure

d = diffusion coefficient of water vapor

D = rainfall duration

E = collision efficiency

E_W = saturation vapor pressure

$f(R_e, P_r')$ = ventilation factor

G = thermodynamic function

g = gravity

L = latent heat of condensation

M = mass of flux

m = mass

m_W = molecular weight of water

P = pressure

q = mixing ratio

q_s = saturation mixing ratio

r = radius of droplets

R = radius of relatively large drops

R_c = critical radius

R_d = gas constant for dry air

S' = supersaturation due to solution effect

S = natural supersaturation, a function of droplet concentration and updraft velocity

t = time

T = temperature

T_e = environmental temperature

V = terminal velocity of drop

V_c = critical terminal velocity

w = liquid water content

W = updraft velocity

x = mole fraction

z = height above cloud base

α = entrainment proportionality constant

ε = the ratio of the molecular weight of water to dry air

γ = surface tension

κ = thermal conductivity of the air

ρ = air density

ρ_e = environmental air density

ρ_L = density of water

σ = virtual mass coefficient

μ = entrainment

APPENDIX B

```
      PROGRAM DURHAM3 (INPUT,OUTPUT)
      REAL LWC, NO
      INTEGER TDELTA
      READ 1000, NCASES
 1000 FORMAT(I5)
      DO 1 J=1,NCASES
      PRINT 9002
 9002 FORMAT(1H1)
      AVVRAD=MEAN VOLUME RADIUS
      R=SEEDING DENSITY (NO/LITER)
      E=COLLISION EFFICIENCY
      GL=GRAVITY (CM/SEC**2)
      LWC=LIQUID WATER CONTENT (GM/M**3)
      RAD=DROP RADIUS
      RL=DROPLET RADIUS
      RD=GAS CONSTANT
      VR (VLR)=TERMINAL VELOCITY OF DROP (DROPLET)
      WL1=LIQUID WATER CONTENT (GM/GM)
      WL4=VOLUME OF WATER EXTRACTED BY DROP GROWTH
      WL5=LIQUID WATER CONTENT OF A CLOUD LAYER
      A=1.0
      GL=980.616
      K=50
      LWC=0.0
      NO=0.0
      RD=2.8704E6
      WL4=0.0
      TDELTA=2
      TOTVOL=0.0
      READ 3000, RAD0, WL1, E, RL, B,T, P
 3000 FORMAT(7F10.4)
      RAD=RAD0
      RHOA=(P*1.0E3)/(RD*T)
      RHOA=AIR DENSITY
      WL3=(4.1888*B*RAD**3)/(RHOA*1.0E15)
      VLR=(2.0*RL**2*GL)/(16.5*1.0E4)
      IF (RAD .LT. 700.0) GO TO 5
      VR=24.1660+0.8976672*RAD-302.506E-6*RAD**2+34.1272E-9*RAD**3
      GO TO 6
    5 VR=-17.8951+0.8978996*RAD+6E.4876E-6*RAD**2-367.608E-9*RAD**3
    6 CONTINUE
      SD=VR*0.02
      WL5=WL1*RHOA*SD*1.0E4
      WL6=(WL5/(SD*1.0E4))
      VOL1=4.1888*RAD**3
   10 CONTINUE
      RAD=RAD0
      IF (RAD .LT. 700.0) GO TO 50
      VR=24.1660+0.8976672*RAD-302.506E-6*RAD**2+34.1272E-9*RAD**3
      GO TO 60
   50 VR=-17.8951+0.8978996*RAD+6S.4876E-6*RAD**2-367.608E-9*RAD**3
   60 CONTINUE
      WL5=WL5-WL4
      WL1=(WL5/(SD*RHOA*1.0E4))
      LWC=(WL1*P/T)*348.2063
```

```
      EPRIME=(E*(RAD+RL)**2)/(RAD*RAD)
      DRAD1=A*(EPRIME/(4.0))*WC*(VR-VLR)*TDELTA*1.0E-2
      RAD=RAD+DRAD1
      VOL=4.1888*RAD**3
      TOTVOL=TOTVOL+VOL
      DVOL=VOL-VOL1
      WL2=(4.1888*B*RAD**3)/(RHOA*1.0E15)
      WL4=WL2-WL3
      NO=NO+1.0
      I=MOD(K,50)
      K=K+1
      IF (I) 2,3,2
    3 PRINT 4000, NO, SD, RAD, VOL, DRAD1, WL4, WL1, DVOL
 4000 FORMAT(5X,2F6.2,6F20.7)
    2 CONTINUE
      IF (DRAD1 .LT. 0.1) GO TO 20
      IF (NO .LT. 3000.0) GO TO 10
   20 CONTINUE
      TOTVOL=TOTVOL+(3000.0-NO)*VOL
      AVVOL=(TOTVOL/3000.0)
      AVRAD=(AVVOL/4.1888)**.333333
      PRINT 4000, NO, SD, AVVOL, AVRAD, WL1
    1 CONTINUE
      END
```

APPENDIX C

NUMERICAL MODEL

```
      PROGRAM DURHAM2 (INPUT,OUTPUT,TAPE1)
      DIMENSION ED(20,6), RADL(20), RDSM(6)
      DIMENSION IDATA(50,8)
      COMMON ZPR(750), TEMP(750), RLIT(750), WATER1(750), WUP(750)
      COMMON WDOTUP(750), ENMIX(750), CLDMIX(750), PRES(750), TVEUP(750)
      REAL K, L, N, LWC, NO, LF, ITIN
      NDIMEN=750
      READ 8002, (RADL(I), I=1,20)
 8002 FORMAT(16F5.0)
      READ 8002, (RDSM(I), I=1,6)
      READ 8002, ((ED(I,J), J=1,6), I=1,20)
      READ 8000, NCASES,NTIMESX
 8000 FORMAT(2I5)
      CPHTOT=0.0
      TOTPREC=0.0
      TOTEFF=0.0
      CC=0.0
      DO 500  J=1,NCASES
      READ 8001, WSTRT, ZNOSTRT, RADSTRT, RADS, PRO, SD, BSTRT
 8001 FORMAT(10X,7F10.4)
      IHR=0
      IKT=1
   22 READ (1) (IDATA(IKT,IJ), IJ=1,8)
      IF (EOF(1)) 26, 24
   24 IF (IDATA(IKT,3) .NE. IHR) GO TO 22
      IKT=IKT+1
         IF(IKT.GT.50)  STOP 24
      GO TO 22
   26 CONTINUE
      IKT=IKT-1
C******  CHECKING FOR MISSING RH VALUES INSIDE THE SOUNDING.  *******
      LO=1
 2224 DO 25 ICK =LO,IKT
      IF (IDATA(ICK,7) .EQ. 0) GO TO 2225
   25 CONTINUE
      GO TO 2230
 2225 CONTINUE
      NNN=ICK
 2226 ICK=ICK+1
      IF(IDATA(ICK,7) .NE. 0) GO TO 2228
      IF ((ICK-NNN) .GT. 3) GO TO 2230
      GO TO 2226
 2228 IHI=ICK-1
      IRH=((IDATA(NNN-1,7)+IDATA(ICK,7))+.5)/2.
         DO 2229 IKC=NNN,IHI
      IDATA(IKC,7) = IRH
 2229 CONTINUE
      LO=ICK    %    IF(ICK.GE.IKT) GO TO 2230
      GO TO 2224
 2230 CONTINUE
         IF(NTIMESX.EQ.0) NTIMESX=1
         DO 500 NTIME2=1,NTIMESX
      IF (NTIME2 .GT. 1) READ 8001, WSTRT, ZNOSTRT, RADSTRT, RADS, PRO,
     1 SD, BSTRT
      DO 13 I=1,750
```

```
      TVEUP(I)=0
      ZPR(I)=0
      TEMP(I)=0
      RLIT(I)=0
      WATFR1(I)=0
      WUP(I)=0
      WOOTUP(I)=0
      ENMIX(I)=0
      CLDMIX(I)=0
      PRES(I)=0
   10 CONTINUE
      PRINT 9002
 9002 FORMAT(/////)
*********INITIALIZE DATA*****************************************
      B=BSTRT
      W0=WSTRT
      ZNO=ZNOSTRT
      RAD=RADSTRT
      CP=1.0048E7
      DH=10.0
      E=0.0
      ECON=2.71828
      EPRIME=0.0
      EE=0.0
      F=1.0026
      FF=0.0
      GL=980.616
      H=IDATA(1,5)
      T0=0
      ISUB=1
      ISTART=1
      ITIM=0
      JTIM=60
      LP=0.0
      LTIM=0.0
      LWC=0.0
      M0=18.0
      R=8.31436E7
      RAD1=0.0
      RD=2.8704E6
      RHOA0=1.2047767E-3
      RL=0.0
      RWE=0.0
      RWF=0.0
      SOC=0.0
      SPRIME=0.0
      TDELTA=2
      TIME=0.0
      U=0.0
      U1=0.0
      WL=0.0
      WL1=0.0
      WL2=0.0
      WL7=0.0
      Z=0.0
```

```
      ZDELTA=0.0
      ZLT=0.0
      CON=0
      H=H+200.0
      CR=500.0
********DETERMINE CLOUDBASE--CCL*****************************
      JKT=1
   28 JKT=JKT+1
******** EXIT FROM CALCULATIONS IF TOP SOUNDING IS PASSED.  ********
         IF(JKT.GT.IKT) GO TO 500
      IF ((IDATA(JKT,5)*1.0) .LT. H) GO TO 28
      IF (IDATA(JKT,8) .LT. 0) IDATA(JKT,8)=0
      HDELTA=H-IDATA(JKT-1,5)
      HTDIFL=IDATA(JKT,5)-IDATA(JKT-1,5)
      PCT=HDELTA/HTDIFL
      TE=IDATA(JKT-1,6)*.1+((IDATA(JKT,6)-IDATA(JKT-1,6))*0.1)*PCT
      T=(TE+IDATA(JKT,6)*0.1)/2.0
      P=ECON**(ALOG(IDATA(JKT-1,4)*1.0)-(GL*HDELTA)/(2.8704E4*T))
      T=TE
      RH=IDATA(JKT-1,7)*0.01*((IDATA(JKT,7)-IDATA(JKT-1,7))*0.01)*PCT
      EWP=6.11*10.0**(7.5*(T-273.0)/(T-35.7))
      RWP=((0.62197*EWP*F)/(P-EWP*F))*RH
      EWE1=6.11*10.0**(7.5*(TE-273.0)/(TE-35.7))*RH
      L=(2500.537-(2.369*(TE-273.16)))*1.0E7
      TW=-ALOG(EWE1/6.1078)*(R/(18.0*L))+1.0/273.0
      TW=1.0/TW
                  EN=0.15/CR
      PRINT 34, PCT, T, TE, HDELTA, P, RH, DT, RWP, HTDIFL, JKT,
     1IDATA(JKT,7), IDATA(JKT-1,7)
   34 FORMAT(2X,9F10.5,3I8)
      GO TO 31
   27 JKT=JKT+1
******** EXIT FROM CALCULATIONS IF TOP SOUNDING IS PASSED.  ********
         IF(JKT.GT.IKT) GO TO 500
   31 CONTINUE
      IF ((IDATA(JKT,5)*1.0) .LT. H) GO TO 27
                  EN=0.15/CR
      CR=CR+0.40*DH
      HDELTA=H-IDATA(JKT-1,5)
      HTDIFL=IDATA(JKT,5)-IDATA(JKT-1,5)
      PCT=HDELTA/HTDIFL
      TE=IDATA(JKT-1,6)*.1+((IDATA(JKT,6)-IDATA(JKT-1,6))*0.1)*PCT
      RH=IDATA(JKT-1,7)*0.01*((IDATA(JKT,7)-IDATA(JKT-1,7))*0.01)*PCT
      H=H+DH
      IF (H .GT. 6000.0) GO TO 399
      P=EXP(ALOG(P)-(GL*DH)/(2.8704E4*T))
      DT=-(GL/CP+0.01*EN*(T-TE))*100.0*DH
      T=T+DT
      EW=6.11*10.0**(7.5*(T-273)/(T-35.7))
      EWE=6.11*10.0**(7.5*(TE-273.0)/(TE-35.7))*RH
      EWE1=(EWE1+EWE*EN*DH)/(1.0+EN*DH)
      TW=-ALOG(EWE1/6.1078)*(R/(18.0*L))+1.0/273.0
      TW=1.0/TW
      IF (TW .LE. TE) GO TO 31
  399 CONTINUE
```

```
      PRINT 34, H, T, TE, P, TW, RWF, EWF1, PH, EWF, JKT, IDATA(JKT,7),
     1IDATA(JKT-1,7)
      IF (H .GT. 6000.0) GO TO 499
      CRH=H
      HDELTA=CRH-IDATA(JKT-1,5)
      HTDIFL=IDATA(JKT,5)-IDATA(JKT-1,5)
      PCT=HDELTA/HTDIFL
      TE=IDATA(JKT-1,6)*.1+((IDATA(JKT,6)-IDATA(JKT-1,6))*0.1)**PCT
      T=(TE+IDATA(JKT,6)*0.1)/2.0
      P=ECON**(ALOG(IDATA(JKT-1,4)*1.0)-(GL*HDELTA)/(2.8704E4*T))
      RH=IDATA(JKT-1,7)*0.01+((IDATA(JKT,7)-IDATA(JKT-1,7))*0.01)*PCT
      IF (IDATA(JKT,8) .LT. 0) IDATA(JKT,8)=0
      W0=((IDATA(JKT-1,8)+(IDATA(JKT,8)-IDATA(JKT-1,8))*PCT)*100.0
         IF(W0.LT.0.) W0=0.
      W1=W0
      CR=2*PR0
      CR0=CR
      W=W0
      T=TE
      PR=PR0
      W1=0.0
      PHOA=(P*1.0E3)/(RD*T)
      IF (RADS .EQ. 0.0) GO TO 10
      RAD=1.911*RADS
      GO TO 10
    9 CONTINUE
      TDELTA=2.0
      I0=I2+1
   10 KK=MOD(LTIM,JTIM)
      NRL=0
      NRS=0
      ISUB=1
      N=1.8325E-4*(416.16/(T+120.0))*(T/296.16)**1.5
      IF (KK .NE. 0) GO TO 15
      TIME=ITIM/60.0
      PRINT 9000, TIME, RAD, RL, Z, T, P, W, LWC, PR
      PRINT 9000, TIME, PERF, RWF, TV, TVE, TEMPD, WDOT, RW, RWE
 9000 FORMAT(5X, F6.2,8(F15.4))
   15 IF (RL .LT. 700.0) GO TO 20
      VLR=24.1660+0.8976672* RL-302.506E-6*RL**2+34.1272E-9*RL**3
      GO TO 40
C********CALCULATE DROPLET TERMINAL VELOCITY ******************
   20 IF (RL .LE. 50.0) GO TO 30
      VLR=-17.8951+0.8978996*RL+65.4876E-6*RL**2-367.608E-9*RL**3
      GO TO 40
   30 VLR=(2.0*RL**2*GL)/(16.5*1.0E4)
   40 IF (RAD .LT. 700.0) GO TO 50
      VR=24.1660+0.8976672*RAD-302.506E-6*RAD**2+34.1272E-9*RAD**3
      GO TO 41
C********CALCULATE DROP TERMINAL VELOCITY**********************
   50 IF (RAD .LE. 50.0) GO TO 100
      VR=-17.8951+0.8978996*RAD+65.4876E-6*RAD**2-367.608E-9*RAD**3
      GO TO 41
  100 VR=(2.0*RAD**2*GL)/(16.5*1.0E4)
   41 NRL=NRL+1
```

```
      IF (RAD .GE. RADL(NRL)) GO TO 41
   51 NRS=NRS+1
      IF (RL .GE. RDSM(NRS)) GO TO 51
      E=ED(NRL,NRS)
      RHOA1=RHOA
      RHOA=(P*1.0E3)/(RD*T)
      VLR=VLR*(RHOA0/RHOA)**0.4
      VR=VR*(RHOA0/RHOA)**0.4
      IF (W .GT. VR) TDELTA=2.0
      TVE=(1.0+0.61*RWE)*TE
      L=(2500.537-(2.369*(T-273.16)))*1.0E7
      WL2=(4.1888*B*RAD**3)/(RHOA*1.0E15)
      ZDELTA=(W-VR)*TDELTA*1.0E-2
      LTIM=LTIM+2
      IF (ZLT .GE. 1.0) GO TO 700
      DUR=200.0*(Z/VR)+360
      TTOP=ITIM
      IMAX=I0
  700 IF (ZDELTA .LE. 0.0) GO TO 800
      Z=Z+ZDELTA
      JKT=0
      H=CBH+Z
   57 JKT=JKT+1
C******* EXIT FROM CALCULATIONS IF TOP SOUNDING IS PASSED.  **********
      IF(JKT.GT.IKT) GO TO 500
C********* CLOUD PHYSICS CALCULATIONS MADE ON ASCENT ***********
      IF ((IDATA(JKT,5)*1.0) .LT. H) GO TO 57
      HDELTA=H-IDATA(JKT-1,5)
      P=ECON**(ALOG(P)-(GL*ZDELTA)/(2.8704E4*T))
      HTDIFL=IDATA(JKT,5)-IDATA(JKT-1,5)
      PCT=HDELTA/HTDIFL
      TE=IDATA(JKT-1,6)*.1+((IDATA(JKT,6)-IDATA(JKT-1,6))*0.1)*PCT
      RH=IDATA(JKT-1,7)*0.01+((IDATA(JKT,7)-IDATA(JKT-1,7))*0.01)*PCT
      IF (IDATA(JKT,8) .LT. 0) IDATA(JKT,8)=0
      U=(IDATA(JKT-1,8)+(IDATA(JKT,8)-IDATA(JKT-1,8))*PCT)*100.0
         IF(U.LT.0.) U=0.
         IF(I0.GT.NDIMEN)    STOP 225
      I0=I0+1
      ZPR(I0)=Z
                    EN=0.15/CR
                   ENP=0.15/PR
      EW=6.11*10.0**(7.5*(T-273)/(T-35.7))
      RW=((0.62197*EW*F)/(P-EW*F))
      CLDMIX(I0)=RW
      EWE=6.11*10.0**(7.5*(TE-273)/(TE-35.7))
      RWE=((0.62197*EWE*F)/(P-EWE*F))
      RWE=RH*RWE
      ENMIX(I0)=RWE
      TVE=(1.0+0.61*RWE)*TE
      TVEUP(I0)=TVE
C********FREEZING OF CLOUD WATER ******************************
      IF (T-253.0) 2, 2, 3
    2 PERF=EXP(-(T-233.0)/7)
      IF (PERF .GE. 1.0) PERF=1.0
      RWF=PERF*RW-RWF
```

```
      IF (RWF .LT. 0.0) RWF=0.0
      IF (PERF .GE. 1.0) RWF=0.0
      LF=(288.89-2.847*(253.0-T))*1.0E7
    3 CONTINUE
      TEMPD=-((GL/CP)*(1+(L*RW)/(RD*T))+0.01*(EN**(T-TE)-(LF/CP)*
     1(RWE/(ZDELTA*100.0))+EN*(L/CP)*(RW-RWE)))*100.0*ZDELTA/
     2(1.0+(0.622*L**2*RW)/(CP*RD*T**2))
      T=T+TEMPD
      TEMP(I0)=T
      TV=(1.0+0.61*RW)*T
      K=2.43*1.0E3*(393.16/(T+120.0))*(T/273.16)**1.5
      PRES(I0)=P
      D=0.226*(T/273.16)**1.81*(1000.0/P)
      EW=6.11*10.0**(7.5*(T-273)/(T-35.7))
      RW2=((0.62197*EW*F)/(P-EW*F))
      RHOV=(RW2*P/T)*0.0003482063
      G=((D*RHOV))*(1.0+(D*L**2*RHOV*W0)/(R*T**2*K))**(-1)
      FE=FE+(RW-RW2)*RHOA*314.159*ZDELTA*RR**2
      WL1=WL7
      WL1=(WL1*(RW-RW2))*(1.0/(1.0+EN*ZDELTA))-EN*ZDELTA*(RW-RWE)
      IF (WL1 .LT. 0.0001) WL1=0.0001
      WATER1(I0)=WL1
      WL=WL1+WL2
      WL7=WL1
      IF (B .LT. 10.0) GO TO 398
      ZNO=ZNOSTRT+B*1.0E-3
      RAD2=(RAD-RAD1)*(25.0*SD)/VR+RAD1
      WL1=WL1-R**4.1888E-15*(RAD2**3-RAD1**3)/RHOA
      IF (WL1 .LT. 0.0) WL1=0.0001
  398 CONTINUE
      NO=ZNO/RHOA
      RL=(WL1/(4.1888*NO))**.33333*1.0E4
      LWC=(WL1*P/T)*348.2063
      W1=W
********* CALCULATE UPDRAFT ACCELERATION AND VELOCITY *********
      WDOT=((TV-TVE)/(TVE)-WL)*653.764-ENP*W**2*1.0E-2
      WDOTUP(I0)=WDOT
      W=W+WDOT*TDELTA
      U1=(U1+EN*U*ZDELTA)/(1.0+EN*ZDELTA)
      WWW=(W**2-(U1-U0)**2)
         IF(WWW.LE.0.0) GO TO 327
      W=SQRT(WWW)
  327 CONTINUE
      WUP(I0)=W
      DW=W-W1
      IF (ZLT .GE. 1.0) GO TO 701
      IF ((W+(DW/(W*TDELTA))*(5000.0/(W*TDELTA))) .LE. 0.0) GO TO 204
      IF (W .LE. 0.0) GO TO 204
********* CALULATE CHANGE IN UPDRAFT RADIUS ********************
      DRHOA=RHOA-RHOA1
      DPR=0.1*ZDELTA-(PR/2.0)*(DW/W+DRHOA/RHOA)
      PR=PR+DPR
      IF (PR .GT. CR .OR. CR .GT. CR0) CR=PR
  701 CONTINUE
      RLIT(I0)=RL
```

```
      SIGMAR=NO*RL*1.0E-4
      STD=(0.0239*W+NO*1.72E-6)/SIGMAR
      TD2=T+STD
      EW2=6.11*10.0**(7.5*(TD2-273)/(TD2-35.7))
      SPRIME=(EW2/EW)-1.0
      IF (FF .GT. 0.999) GO TO 310
      X=0.23271*RAD**3
      Y=0.310307*RADS**3
      FF=X/(X+Y)
      IF (FF .GT. 0.91) GO TO 317
      FF=FF-.715*(0.91-FF)
  317 S=SPRIME+1.0/FF-1.0
      GO TO 777
  310 CONTINUE
      S=SPRIME
  777 CONTINUE
      GO TO 802
  800 DW=W1-W
********CALCULATIONS MADE WHEN DROP IS FALLING RELATIVE TO CLOUDBASE**
      L=(2500.537-(2.369*(TE-273.16)))*1.0E7
      JTIM=600
      ZLT=ZLT+1.0
      TDELTA=(50.0*SD)/VR
          IF (TDELTA .GT. 30.0) TDELTA=30.0
      ZDELTA=(W-VR)*TDELTA*1.0E-2
         IF(ZDELTA.GE.0.0) GO TO 9
      Z=Z+ZDELTA
*********INTERPELATES DATA FED INTO ARRAYS ON ASCENT **********
      DO 12 IZ=ISTART,IMAX
      I2=IMAX+1-IZ
      IF (Z-ZPR(I2)) 12,11,11
   12 CONTINUE
   11 CONTINUE
      IF (I2 .GE. IMAX) I2=IMAX-1
         IF(I2.LE.0)  I2=1
      WL1=WATER1(I2)+((WATER1(I2)-WATER1(I2+1))/(ZPR(I2)-ZPR(I2+1)))*
     1(Z-ZPR(I2))
      IF (WL1 .LT. 0.0001) WL1=0.0001
      TVE=TVEUP(I2)+((TVEUP(I2)-TVEUP(I2+1))/(ZPR(I2)-ZPR(I2+1)))*
     1(Z-ZPR(I2))
      RWE=ENMIX(I2)+((ENMIX(I2)-ENMIX(I2+1))/(ZPR(I2)-ZPR(I2+1)))*
     1(Z-ZPR(I2))
      WO=WUP(I2)+((WUP(I2)-WUP(I2+1))/(ZPR(I2)-ZPR(I2+1)))*
     1(Z-ZPR(I2))
      WDOT=WDOTUP(I2)+((WDOTUP(I2)-WDOTUP(I2+1))/(ZPR(I2)-ZPR(I2+1)))*
     1(Z-ZPR(I2))
      RW=CLDMIX(I2)+((CLDMIX(I2)-CLDMIX(I2+1))/(ZPR(I2)-ZPR(I2+1)))*
     1(Z-ZPR(I2))
      P=PRES(I2)+((PRES(I2)-PRES(I2+1))/(ZPR(I2)-ZPR(I2+1)))*
     1(Z-ZPR(I2))
      NO=ZNOSTRT/RHOA
      RL=(WL1/(4.1888*NO))**.33333*1.0E4
      IF (W .GT. 0.0) GO TO 17
      TEMPD=-((GL/CP)*(1+(L*RW)/(RD*T))+0.01*(ENP*(T-TE)+EN*(L/CP)*
     1(RW-RWE)))*100.0*ZDELTA/(1.0+(0.622*L**2*RW)/(CP*RD*T**2))
```

```
      T=T+TEMPD
      TV=(1.0+0.61*RW)*T
      GO TO 14
   17 CONTINUE
      T=TEMP(I2)+((TEMP(I2)-TEMP(I2+1))/(ZPR(I2)-ZPR(I2+1)))*
     1(Z-ZPR(I2))
      TV=(1.0+0.61*RW)*T
   14 ISTART=IMAX-I2-10
      IF (ISTART .LT. 1)   ISTART=1
      LWC=(WL1*P/T)*348.2063
         RAD1=RAD
         IF (RAD .GT. 3000.0) RAD=3000.0
      WF=(300.0/(CON*SD))*EXP(-2.0*(RAD/2000.0)**2)
         RAD=RAD1
      IF (WF-1.0) 4, 4, 5
    4 LWC=WF*LWC
    5 CONTINUE
      IF (W .LT. 0.0) GO TO 111
      IF (WDOT .LT. 0.0) GO TO 555
      WDOT=WDOT-WL2*653.744
      IF (WDOT .LT. 0.0) GO TO 999
      GO TO 666
  555 CONTINUE
      WDOT=WDOT+WL2*653.744
  666 CONTINUE
      W=W0-WDOT*TDELTA
      GO TO 802
  111 WDOT=((TV-TVE)/(TVE)-WL1-WL2)*653.744
  999 CONTINUE
      W=W0+WDOT*TDELTA
  802 CONTINUE
      EPRIME=(E*(RAD+RL)**2)/(RAD*RAD)
      IF (RADS) 202, 201, 202
  201 IF (RAD .GT. 45.0) GO TO 202
      A=1.82
      GO TO 203
  202 A=1.0
  203 CONTINUE
******** CALCULATE DROP GROWTH ***********************************
      RAD1=RAD
      DRAD1=A*(EPRIME/(4.0))*LWC*(VR-VLR)*TDELTA*1.0E-2
      DRAD2=RAD
      DRAD3=(2.*G*S*TDELTA*1.0E8*RAD**2)
         IF(DRAD3.GE.0) DRAD2=SQRT(DRAD3)
      RAD=DRAD1+DRAD2
      IF (T .LE. 243.0) GO TO 207
      IF (T .LT. 273.0 .AND. SOC .GT. 1.0) GO TO 207
      IF (T-243.0) 208, 208, 209
  208 SOC=2.0
  209 IF (RAD .LT. 3.06E9/VR**2) GO TO 207
      RAD=RAD*0.5
      ISUB=1
      B=4.0*B
      CON=3.5*CON
  207 ITIM=ITIM+TDELTA
```

```
      IF (Z .GT. 0.0) GO TO 10
  204 TIME=ITIM/60.0
      PRECIP=R*RAD**3*PR0**2*SD*1.06E-17
      EE2=EE/1.273E3
      EE21=EE2*(DUR/TTOP)*EE2
      EFF=PRECIP/EE2
      EFF1=PRECIP/EE21
      EFF2=(EFF+EFF1)/2.0
      DUR=DUR/60.0
      PRINT 9000, TIME, RAD, Z, T, W, DUR, EFF2, PRECIP
      PRINT 9000, TIME, RWF, PERF, LF, TEMPD, WDOT, CON, WL2
      TOTPREC=TOTPREC+PRECIP
      CBHTOT=CBHTOT+CBH
      TOTEFF=TOTEFF+EFF2
      CC=CC+1.0
      AVCBH=CBHTOT/J
    1 FORMAT(5X,5F25.3)
      PRINT 1, TOTPREC, TOTEFF, CC, AVCBH, CBHTOT
  499 CONTINUE
  500 CONTINUE
      END
```

APPENDIX D

AVERAGED SOUNDINGS FOR VARIOUS STATIONS

AVERAGE SOUNDING FOR COLUMBIA

Pressure (mb)	Height (m)	Temperature (^{o}K)	Relative Humidity	Wind Speed (ms^{-1})
986	237	302.7	51	4
950	570	298.5	53	5
900	1047	294.6	58	5
850	1540	291.1	56	6
800	2057	288.1	48	6
750	2598	285.0	43	7
700	3177	281.6	42	8
650	3782	277.9	39	8
600	4434	274.4	35	9
550	5121	270.0	33	9
500	5877	265.5	31	10
450	6086	260.4	28	11
400	7580	254.3	26	12
350	8562	247.5	26	15
300	9662	239.2	25	16
250	10916	229.7	1	18
200	12385	219.6	0	19
175	13235	214.7	0	19
150	14195	210.2	0	17
125	15308	206.7	0	13
100	16660	207.5	0	8
75	17977	211.3	0	5
50	18860	213.2	0	4

AVERAGE SOUNDING FOR FORTH WORTH

Pressure (mb)	Height (m)	Temperature (^{o}K)	Relative Humidity	Wind Speed (ms^{-1})
993	164	306.4	41	4
950	581	302.3	42	6
900	1057	298.0	47	6
850	1555	293.7	53	5
800	2076	289.5	55	5
750	2620	286.1	48	5
700	3201	282.7	43	4
650	3810	279.1	41	5
600	4465	275.2	40	5
550	5160	271.3	35	6
500	5916	267.1	30	6
450	6733	262.0	28	6
400	7631	256.0	28	7
350	8619	248.9	25	8
300	9726	240.6	24	9
250	10986	230.7	2	11
200	12459	219.3	0	12
175	13305	213.3	0	12
150	14256	207.4	0	11
125	15351	202.9	0	8
100	1667	203.5	0	7
75	18020	207.6	0	6
50	18838	210.4	0	7

AVERAGE SOUNDING FOR DENVER

Pressure (mb)	Height (m)	Temperature (°K)	Relative Humidity	Wind Speed (ms^{-1})
839	1016	306.5	36	5
800	2036	296.5	32	6
750	2592	291.9	35	4
700	3182	286.8	40	4
650	3799	281.7	45	4
600	4458	276.4	50	6
550	5148	271.0	55	7
500	5908	265.9	56	9
450	6718	261.0	49	10
400	7615	255.2	41	11
350	8601	248.5	35	13
300	9706	240.3	32	16
250	10964	230.6	4	19
200	12420	220.0	0	20
175	13263	214.5	0	19
150	14240	208.9	0	17
125	15344	205.1	0	13
100	16683	206.1	0	7
75	18049	210.7	0	4
50	18881	213.0	0	4

AVERAGE SOUNDING FOR RAPID CITY

Pressure (mb)	Height (m)	Temperature (°K)	Relative Humidity	Wind Speed (ms^{-1})
904	964	301.0	42	5
900	1017	299.6	42	5
850	1511	295.6	42	6
800	2036	291.4	45	5
750	2582	287.4	46	6
700	3165	283.2	46	7
650	3772	278.7	44	9
600	4426	273.9	40	11
550	5110	269.1	38	12
500	5867	264.3	35	14
450	6671	258.9	32	16
400	7560	252.7	29	18
350	8535	245.5	29	20
300	9627	237.6	27	24
250	10873	228.8	0	28
200	12306	220.2	0	30
175	13146	216.4	0	28
150	14154	212.3	0	25
125	15281	209.8	0	18
100	16652	210.6	0	11
75	17985	213.8	0	5
50	18878	215.2	0	3

BIBLIOGRAPHIC DATA SHEET	1. Report No. CSU-ATSP-202	2.	3. Recipient's Accession No.
4. Title and Subtitle WARM CUMULUS CLOUD SEEDING POTENTIAL			5. Report Date July 1973 6.
7. Author(s) Richard Durham			8. Performing Organization Rept. No. CSU-ATSP-202
9. Performing Organization Name and Address Department of Atmospheric Science Colorado State University Fort Collins, Colorado 80521			10. Project/Task/Work Unit No. 11. Contract/Grant No. NSF GI-31460
12. Sponsoring Organization Name and Address National Science Foundation Washington, D.C.			13. Type of Report & Period Covered Project Report 14.

15. Supplementary Notes

16. Abstracts

A one-dimensional steady-state cumulus model is described. The model considers the processes of lateral entrainment, droplet growth by condensation and coalescence, droplet freezing and the development and fallout of precipitation, as well as the standard thermodynamic and dynamic processes in isolated cumuli. The numerical model is reviewed and comparisons are made between model predicted cloud characteristics and observations made during a cumulus modification program conducted near Rapid City, South Dakota in the summer months of 1969-1971. The model is used to evaluate the importance of the warm coalescence process and the climatological potential for rainfall augmentation through sodium chloride seeding of isolated cumulus clouds on the Great Plains. The model shows that coalescence plays an important role in the natural formation of rain in the southeastern portions of the Great Plains, but is of minor importance in the more continental areas. Rainfall could be initiated by sodium chloride seeding in all areas of the Great Plains. In the southern portions of the Great Plains significant amounts of rain could be produced in clouds that are unsuitable for other forms of seeding.

17. Key Words and Document Analysis. 17a. Descriptors

Cumulus Model	551.576.1
Warm Cloud Seeding	551.577.1
Cloud Droplet Growth	551.578.4
Seeding Potential	551.578.11

17b. Identifiers/Open-Ended Terms

17c. COSATI Field/Group

18. Availability Statement	19. Security Class (This Report) UNCLASSIFIED	21. No. of Pages 84
	20. Security Class (This Page UNCLASSIFIED	22. Price